

## SN 1961V: A PULSATONAL PAIR-INSTABILITY SUPERNOVA

S. E. WOOSLEY<sup>1</sup> AND NATHAN SMITH<sup>2</sup>

*Draft version May 16, 2022*

### ABSTRACT

We explore a variety of models in which SN 1961V, one of the most enigmatic supernovae (SNe) ever observed, was a pulsational pair-instability supernova (PPISN). Successful models reproduce the bolometric light curve of the principal outburst and, in some cases, the emission one year before and several years afterward. All models have helium-rich ejecta, bulk hydrogenic velocities near 2000 km s<sup>-1</sup>, and total kinetic energies from 4 to 8 × 10<sup>50</sup> erg. Each eventually leaves behind a black hole remnant. Three subclasses of PPISN models are explored, each with two different choices of carbon abundance following helium burning. Carbon is an important parameter because shell carbon burning can weaken the explosion. The three subclasses correspond to situations where SN 1961V and its immediate afterglow were: a) a single event; b) the first of two or more pulsational events separated by decades or centuries; or c) the latter stages of a complex explosion that had already been going on for a year or more. For the low carbon case, the main sequence mass for SN 1961V’s progenitor would have been 100 to 115 M<sub>⊙</sub>; its pre-SN helium core mass was 45 to 52 M<sub>⊙</sub>; and the final black hole mass, 40 to 45 M<sub>⊙</sub>. For the high-carbon case, these values are increased by roughly 20 to 25%. In some PPISN models, a ∼ 10<sup>40</sup> erg s<sup>-1</sup> star-like object could still be shining at the site of SN 1961V, but it has more likely been replaced by a massive accreting black hole.

*Subject headings:* stars: massive, evolution, supernova, black holes; supernova individual: SN 1961V

### 1. INTRODUCTION

Few supernovae (SNe) have histories rivaling the rich, controversial case of SN 1961V in the nearby (∼10 Mpc) spiral galaxy NGC 1058. Discovered in July, 1961 by Wild (1961), the event was originally classified by Zwicky (1964) as a Type V SN. It was, for a time, the prototypical “supernova impostor”, noted, in particular, for its similarity to Eta Carinae (Zwicky 1964; Goodrich et al. 1989; Filippenko et al. 1995; Humphreys et al. 1999). In fact, Eta Carinae was Zwicky’s only other Type V SN. The progenitor was first seen as a 19th magnitude object starting in 1937, and repeatedly visited by observers thereafter (Bertola 1964; Zwicky 1964). An appreciable rise in brightness by roughly a factor of 10 was reported in November 1960, about a year before the SN. During the “main event” in late 1961, the irregular luminosity exceeded, for a time, that of a typical Type II SN. Overall, the light curve of this main event was extremely unusual among known SNe, with a ∼100 day plateau resembling a typical SN II-P at an absolute magnitude of roughly −16.5 mag, punctuated by a late, brief luminosity spike at almost −18 mag. The decline from this last peak was slow and unsteady over the subsequent decade.

Given the large inferred luminosity of the star before it exploded, Goodrich et al. (1989) suggested a zero-age main-sequence (ZAMS) mass of over 240 M<sub>⊙</sub> and a pre-outburst mass of over 170 M<sub>⊙</sub>. Their estimated absolute magnitude, −12.1 mag, relied on an uncertain extinction correction of 0.6 mag though, and the star could have been fainter, or multiple.<sup>3</sup> Kochanek et al. (2011) later

reduced the lower limit for the mass to 80 M<sub>⊙</sub> and assigned a metallicity ∼1/3 solar. Even then, the SN progenitor was one of the brightest stars in NGC 1058 and clearly quite massive. A very high-mass progenitor is reasonable based on its local environment, since SN 1961V resides within a young giant H II region (Goodrich et al. 1989; Filippenko et al. 1995; Van Dyk et al. 2002; Chu et al. 2004). The measured helium to hydrogen ratio in the SN ejecta was at least 4 times solar (Branch & Greenstein 1971). Observations showed that the SN returned to approximately its pre-SN brightness from about 1.5 to 4 years after its peak (Bertola & Arp 1970), but then continued to fade steadily afterward. By seven years after its peak, the source at SN 1961V’s position declined to ∼3 mag fainter than the progenitor at visual wavelengths (Bertola & Arp 1970), and after 4 decades it had faded to about 7 mag fainter than the progenitor.

The SN, if it was one, definitely had some unexpected physical characteristics (Bertola 1964; Zwicky 1964; Branch & Greenstein 1971). Its expansion velocity, measured from line widths in its spectra, was unusually slow compared to most SNe II of similar luminosity. Zwicky (1964) reported a speed, based on H $\alpha$  near peak, of about 3700 km s<sup>-1</sup>, but noted the presence of many narrower lines and commented that the “true expansion speed” was probably slower. Branch & Greenstein (1971) estimated ∼ 2000 km s<sup>-1</sup> from fitting the entire spectrum, and Goodrich et al. (1989) estimated 2100 km s<sup>-1</sup> from analysis of H $\alpha$  at late times. The spectrum was not like that of common Type I or II SNe (Branch & Greenstein 1971). If the same event were discovered today, it would most likely be classified as Type IIn, but that designation did not exist at the time (see Smith et al. 2011). The main light curve shape was unusual and irregular. The SN had long-lasting precursor emission, and its post-peak decline lasted many years, with several late peaks and plateaus as it faded. The inferred

<sup>1</sup> Department of Astronomy and Astrophysics, University of California, Santa Cruz, CA 95064; woosley@ucolick.org

<sup>2</sup> Steward Observatory, University of Arizona, 933 N. Cherry Ave., Tucson, AZ 85721, USA

<sup>3</sup> Although this is also distance dependent, and modern studies favor a somewhat larger distance than adopted by Goodrich et al.

energetics were also unusual. For an ejecta mass around  $10 M_{\odot}$ , the low velocity implied a low kinetic energy,  $\sim 4 \times 10^{50}$  erg. This is less than the energy of a normal core-collapse SN, but somewhat higher than the inferred energy budget of Eta Carinae’s Great Eruption (Smith et al. 2003). While it had relatively low kinetic energy and was faint except for its brief maximum, the SN’s duration implied a large amount of total radiation. Branch & Greenstein (1971) estimated that the 1961 outburst had an integrated radiated energy of  $\sim 2 \times 10^{50}$  erg. That is, even with substantial errors for distance and bolometric correction, it gave off more light than that radiated by a typical core-collapse SN. Such a large light to kinetic energy ratio is suggestive of a more efficient conversion than in common SN. This, in turn, suggests that the luminosity of SN 1961V was powered, in part, by shock interaction with dense circumstellar material (CSM) or multiple shell collisions (Smith et al. 2011).

The assumption that SN 1961V was a core-collapse SN has frequently been questioned. Often arguing by analogy to Eta Carinae, the outbursts and irregular behavior have been attributed to some sort of stellar variability, often lumped under the rubric of “the outburst of a luminous blue variable (LBV)” (Goodrich et al. 1989; Humphreys et al. 1999). A decades-long debate has raged as to whether the star is still there (Van Dyk et al. 2002; Filippenko et al. 1995; Chu et al. 2004; Smith et al. 2011; Kochanek et al. 2011; Van Dyk & Matheson 2012). A common assumption, which shall later be questioned (§ 5.2), is that, if the star is still there, a SN did not occur. A key point is that if the progenitor was not completely obliterated by the 1961 event, then this rules out a traditional Fe core-collapse SN, but it does not rule out other SN explosion mechanisms like the one we consider here. The LBV hypothesis has in its favor the long and varied history of SN 1961V and its progenitor, which included some outbursts that were well below typical SN luminosities; the low velocity; the peculiar Eta Car-like spectrum; and the temporary return of the luminosity after the 1961 outburst, to values similar to the pre-SN star. On the other hand, the mechanism that drives giant LBV eruptions is not known, and SN 1961V was far more extreme in terms of luminosity and expansion velocity than other LBV eruptions (Smith et al. 2011).

More recently, it has been looking less likely that the pre-SN star survived, though the subject certainly remains controversial and relevant to any modeling. A fading radio source typical of a SN was discovered at the site of SN 1961V, suggesting that this was not just the eruption of a variable star (e.g. Branch & Cowan 1985; Chu et al. 2004). Patton et al. (2019) placed limits on dust obscuration and concluded that, at the present time, any survivor must be much less luminous than the pre-SN star prior to its outburst. Smith et al. (2011) have argued that the velocity and energetics of SN 1961V are not unusual for a SN of Type II<sub>n</sub>. See also Kochanek et al. (2012).

Here we adopt the working hypothesis that SN 1961V was a Type II<sub>n</sub> SN, i.e. the explosive death of a massive star with a residual hydrogen envelope and dense CSM. That death may have been novel and might have taken a long time, but the star is either dead (§ 5.1 and § 5.3) or terminally ill (§ 5.2). A key question then is, if it was a SN, how did it explode? A traditional Fe core collapse

with a single neutrino-driven explosion is not the only way that a massive star can die. Neutrino transport is thought to be insufficiently effective to explode such massive stars (Rahman et al. 2021). A previous SN-based model sidestepped this issue and suggested that SN 1961V was the explosion of a supermassive  $2000 M_{\odot}$  star (Utrobin 1984). Another suggested that SN 1961V was a more common SN (presumably of lower mass) experiencing an unusual amount of CSM interaction (Smith et al. 2011). Both attempted to explain the long duration of the event and its complex time history, the former by a layered structure for the exploding star (Utrobin 1984), the later by a variable circumstellar density (Smith et al. 2010a, 2011). Aside from the obvious issue of whether  $2000 M_{\odot}$  pre-SN stars exist, there is no known mechanism for exploding them. They are expected to collapse directly to black holes (Heger & Woosley 2002; Heger et al. 2003; Rahman et al. 2021). With rotation and progenitors derived from a stellar evolution code, neither the layered structure nor the explosion of a  $2000 M_{\odot}$  model resembled the parametric models of Utrobin (see Ensmann (1989) and Stringfellow as cited in Goodrich et al. (1989)). The model of Smith et al. (2011) was qualitative and lacked a specific explosion or stellar model, but resembles in outcome, what will be discussed here.

Here we explore the consequences of models in which SN 1961V exploded as a pulsational pair-instability supernova (PPISN; e.g. Barkat et al. 1967; Heger & Woosley 2002; Woosley et al. 2007; Woosley 2017). Pastorello et al. (2013) have also speculated that SN 1961V may have been a PPISN, but no specific model was presented. This mechanism can produce long duration, irregular light curves in stars having  $M_{ZAMS}$  comparable to the inferred pre-SN mass. The luminosity of the pre-SN star is roughly consistent with 23 years of observations and, in some cases, the explosion returns to approximately its pre-SN value after the major outburst. The velocity of most of the hydrogen-rich ejecta of PPISN is near  $2000 \text{ km s}^{-1}$  for reasonable hydrogenic envelope masses. PPISN are expected to occur in regions with low metallicity, mainly because of the prodigious mass-loss winds of such luminous stars. The restrictions on low metallicity might be relaxed somewhat, however, due to modern reductions in empirical mass-loss rates (Smith 2014).

Unlike traditional core-collapse SNe — but similar to SNe II<sub>n</sub> — shock interaction with matter ejected in previous pulses or by the pre-SN wind can, in some cases, contribute appreciably to the light curve. Many solar masses of material are available for CSM interaction, and shells typically interact between  $10^{15}$  cm and  $10^{16}$  cm. The helium to hydrogen ratio is naturally very supersolar, and the efficiency for converting kinetic energy to light is high. These are events that should occur in nature and produce black holes with masses like those detected by LIGO (e.g., Abbott et al. 2019). Their explosion characteristics are robust and do not involve neutrino transport.

Complicating our study, though, it turns out that there are three PPISN solutions to SN 1961V, each with different strengths and weaknesses. There are models in which: a) The SN was a singular event in late 1961 lasting of order 200 days during which multiple pulses occurred and the remnant collapsed to a black hole (§ 5.1). In this case, all transient emission before and after the 1961 event requires other explanations, interaction with

a prior wind or LBV-like eruptions being possibilities as inferred in many SNe II<sub>n</sub>, including the remarkable case of SN 2009ip (Smith et al. 2010b). b) The pulsations continued for decades or centuries with a long quiescent interval between. The main outburst of SN 1961V was then just the first one of two major clusters of pulsations. The second, and an eventual collapse to a black hole, would happen much later. In this case, something resembling the pre-SN star could even still be present, along with a fading radio source (§ 5.2). c) The SN actually commenced well in advance of November 1961, and some major bright prior emission was missed by observers at the time. The enduring emission after a year (i.e., after 1962) is due to shells continuing to collide after the SN core has long since collapsed to a black hole (§ 5.3). In all cases, a black hole remnant with 40 to 50  $M_{\odot}$  is the ultimate product.

## 2. THE OBSERVED LIGHT CURVE

The SN 1961V light curve can be divided into four parts: (1) variable pre-SN emission prior to July 1961, (2) a plateau similar to that of a typical SN II-P, lasting about 120 days, (3) a delayed peak about four times brighter lasting about 30 days, and (4) a rapid decline to two additional long plateaus and slow fading thereafter. The distance to NGC 1058 has historically been uncertain, leading to large ranges in the estimated SN luminosity in the literature. Based upon a compromise between similar values of distance moduli deduced from the expanding photosphere method for SN 1969L, which also happened in NGC 1058 ( $m-M = 30.13$  to  $30.25$  mag), and Hubble expansion ( $m-M = 29.77$ ), Smith et al. (2011) recommended a distance modulus of 30.0 which will be adopted here, with an uncertainty of about 0.2 mag. An additional correction for Galactic extinction of 0.3 mag is assumed.

Table 1 then gives the apparent photographic magnitudes Smith et al. (2011) adapted from Zwicky (1964) and Bertola (1964) and the equivalent luminosities, assuming no bolometric correction. Two of the points, on days 1960.641 and 1960.704 are upper bounds to the brightness. The time when the light curve reaches its peak is 1961.943, with a photographic magnitude (approximately equal to the *B*-band magnitude) of 12.50 mag, corresponding to a peak absolute magnitude of  $-17.8$ . All magnitudes prior to 1964.186 have an observational uncertainty of about 0.1 mag, and points after are uncertain to 0.2 mag. The peak luminosity, again ignoring bolometric correction, is

$$\log_{10}(L/L_{\odot}) = 0.4(4.74 - (m_{pg} - 30.3)). \quad (1)$$

The luminosity on the plateau is thus near  $10^{42}$  erg s<sup>-1</sup>, and the peak luminosity is near  $4 \times 10^{42}$  erg s<sup>-1</sup>. The former is typical for SNe II-P on their plateaus (Sukhbold et al. 2016; Smith et al. 2011). Given uncertainties in distance, bolometric correction and extinction, these estimated luminosities could easily be off by 50%.

## 3. PRESUPERNOVA MODELS

### 3.1. Code Physics

The KEPLER code (Weaver, Zimmerman, & Woosley 1978; Woosley et al. 2002) has been used to model PPISN many times (e.g., Woosley 2017; Woosley & Heger 2021)

and the code physics used here is the same as in those previous studies, except where noted in this section. Standard mass loss prescriptions (Nieuwenhuijzen & de Jager 1990; Wellstein & Langer 1999) and opacities were assumed, but the mass-loss rates were multiplied by an adjustable parameter. This parameter, which was always less than one, even after including scaling for a possibly sub-solar metallicity, was adjusted to give pre-SN hydrogen envelope masses in the desired range. More recent studies of mass loss in very massive stars suggest that the mass-loss rates of Nieuwenhuijzen & de Jager (1990) might be overestimates by a factor of order three for such massive stars due the neglect of the effects of clumping (e.g., Smith 2014). The multipliers we use are thus moderate compared to what would be needed in more modern treatments. Revising the mass-loss rate would also have the salutary effect of making PPISN more easily achievable in higher metallicity environments. For now though, the mass-loss rate multiplier is just a reasonable artifice to achieve a desired pre-SN envelope mass. This multiplier is also sensitive to the radius of the star, especially during helium burning and was closer to unity for smaller radii. The radius, in turn, is sensitive to convection physics and surface boundary conditions (see below).

A composition appropriate to one-third solar metallicity was adopted. That is, the initial abundances of hydrogen and helium were 0.719 and 0.276 by mass fraction and those of heavier species were those of Lodders (2003) multiplied by one third. For example, the mass fractions of carbon, nitrogen, oxygen and iron were  $7.8 \times 10^{-4}$ ,  $2.7 \times 10^{-4}$ ,  $2.3 \times 10^{-3}$ , and  $4.2 \times 10^{-4}$ . All calculations employed a large adaptive nuclear reaction network of approximately 300 to 400 species from hydrogen through krypton coupled directly to the stellar structure. Silicon quasiequilibrium was *not* assumed at any time, up to and including iron core collapse. A large network was necessary to accurately follow weak interactions after carbon burning, including those that happen during silicon burning, but it was also necessary to avoid the quasiequilibrium approximation because of the long cool inter-pulse phases, often below  $10^9$ K, in many of the models where silicon had already begun to burn at the center. This is the same approach used by Woosley (2017) and caused no difficulty here.

Standard values were used for the nuclear reaction rates, except for the triple-alpha ( $3\alpha$ ) reaction of helium burning. It is now understood that the presence of carbon in the pre-SN star weakens the pair instability (Farmer et al. 2019, 2020; Woosley & Heger 2021) and changes its outcome. Carbon burning plus neutrino losses is never exoergic in the centers of such massive stars, but carbon shell burning contributes appreciable energy off-center both prior to and during the pulses. This slows the collapse and can, especially in lower mass models, lead to oxygen even igniting stably for a time at the star's center, halting the collapse completely. Eventually the carbon shell burns out and the pulses commence, but fuel and momentum have been diminished. This not only weakens the explosion, but makes the properties of all but the first pulse sensitive to the uncertain mixing that occurs during the interpulse periods. Mixing can bring new carbon down to a mass coordinate of  $\sim 10 M_{\odot}$  where its burning again slows the collapse. Mix-

TABLE 1. SN 1961V LIGHT CURVE

Date (year)	to L <sub>max</sub> (days)	m <sub>pg</sub> (mag)	L (erg s <sup>-1</sup> )	Date (year)	to L <sub>max</sub> (days)	m <sub>pg</sub> (mag)	L (erg s <sup>-1</sup> )	Date (year)	to L <sub>max</sub> (days)	m <sub>pg</sub> (mag)	L (erg s <sup>-1</sup> )
1937.786	-8823.3	18.20	2.10E+40	1961.866	-28.1	13.75	1.26E+42	1962.805	314.8	17.50	4.00E+40
1937.849	-8800.3	18.20	2.10E+40	1961.868	-27.4	13.66	1.37E+42	1962.806	315.2	17.60	3.65E+40
1946.918	-5487.9	18.00	2.52E+40	1961.871	-26.3	13.60	1.45E+42	1962.816	318.9	17.55	3.82E+40
1946.920	-5487.2	18.00	2.52E+40	1961.874	-25.2	13.40	1.75E+42	1962.817	319.2	17.40	4.39E+40
1949.810	-4431.6	18.10	2.30E+40	1961.901	-15.3	13.00	2.52E+42	1962.820	320.3	17.70	3.33E+40
1949.915	-4393.2	17.90	2.77E+40	1961.920	-8.4	12.80	3.03E+42	1962.827	322.9	17.50	4.00E+40
1951.812	-3700.3	17.70	3.33E+40	1961.923	-7.3	13.00	2.52E+42	1962.838	326.9	17.56	3.78E+40
1951.920	-3660.9	17.70	3.33E+40	1961.932	-4.0	12.66	3.45E+42	1962.839	327.3	17.54	3.85E+40
1952.649	-3394.6	17.70	3.33E+40	1961.935	-2.9	12.97	2.59E+42	1962.874	340.0	17.65	3.48E+40
1954.973	-2545.8	18.00	2.52E+40	1961.937	-2.2	12.80	3.03E+42	1962.890	345.9	17.64	3.52E+40
1960.641	-475.6	>17.0	<6.3E+40	1961.940	-1.1	12.70	3.33E+42	1962.896	348.1	17.80	3.03E+40
1960.704	-452.5	>17.0	<6.3E+40	1961.943	0.0	12.50	4.00E+42	1962.915	355.0	17.80	3.03E+40
1960.942	-365.6	15.80	1.91E+41	1961.945	0.7	12.85	2.90E+42	1962.918	356.1	17.73	3.24E+40
1961.539	-147.6	13.50	1.59E+42	1961.951	2.9	12.71	3.30E+42	1962.956	370.0	18.00	2.52E+40
1961.562	-139.2	13.75	1.26E+42	1961.954	4.0	12.90	2.77E+42	1963.041	401.0	18.03	2.45E+40
1961.589	-129.3	14.00	1.00E+42	1961.958	5.5	13.46	1.65E+42	1963.066	410.2	18.10	2.30E+40
1961.591	-128.6	13.90	1.10E+42	1961.980	13.5	14.04	9.68E+41	1963.074	413.1	18.00	2.52E+40
1961.583	-131.5	13.82	1.19E+42	1961.986	15.7	14.20	8.36E+41	1963.148	440.1	18.20	2.10E+40
1961.594	-127.5	13.97	1.03E+42	1962.003	21.9	14.54	6.11E+41	1963.153	442.0	18.34	1.85E+40
1961.597	-126.4	14.06	9.51E+41	1962.011	24.8	15.10	3.65E+41	1963.156	443.0	18.34	1.85E+40
1961.600	-125.3	13.86	1.14E+42	1962.016	26.7	15.25	3.18E+41	1963.227	469.0	19.00	1.00E+40
1961.602	-124.6	13.80	1.21E+42	1962.021	28.5	15.20	3.33E+41	1963.551	587.3	18.30	1.91E+40
1961.608	-122.4	13.92	1.08E+42	1962.022	28.9	15.30	3.03E+41	1963.567	593.2	18.42	1.71E+40
1961.611	-121.3	13.88	1.12E+42	1962.033	32.9	15.35	2.90E+41	1963.586	600.1	18.46	1.65E+40
1961.625	-116.1	14.08	9.33E+41	1962.063	43.8	15.60	2.30E+41	1963.636	618.4	18.41	1.73E+40
1961.627	-115.4	14.02	9.86E+41	1962.066	44.9	15.35	2.90E+41	1963.649	623.1	18.47	1.64E+40
1961.666	-101.2	13.96	1.04E+42	1962.068	45.7	15.60	2.30E+41	1963.666	629.3	18.35	1.83E+40
1961.672	-99.0	14.06	9.51E+41	1962.074	47.8	15.70	2.10E+41	1963.764	665.1	18.47	1.64E+40
1961.674	-98.3	13.98	1.02E+42	1962.075	48.2	15.75	2.00E+41	1963.805	680.1	18.40	1.75E+40
1961.679	-96.4	13.88	1.12E+42	1962.079	49.7	15.70	2.10E+41	1963.833	690.3	18.40	1.75E+40
1961.681	-95.7	13.92	1.08E+42	1962.085	51.9	15.50	2.52E+41	1963.868	703.1	18.40	1.75E+40
1961.682	-95.3	14.00	1.00E+42	1962.090	53.7	15.40	2.77E+41	1963.895	713.0	18.40	1.75E+40
1961.688	-93.1	14.06	9.51E+41	1962.095	55.5	16.00	1.59E+41	1963.942	730.1	18.40	1.75E+40
1961.690	-92.4	13.92	1.08E+42	1962.096	55.9	16.30	1.21E+41	1964.011	755.3	18.45	1.67E+40
1961.690	-92.4	13.60	1.45E+42	1962.101	57.7	15.90	1.75E+41	1964.052	770.3	18.50	1.59E+40
1961.698	-89.5	13.97	1.03E+42	1962.139	71.6	15.80	1.91E+41	1964.090	784.2	18.35	1.83E+40
1961.704	-87.3	13.95	1.05E+42	1962.148	74.9	16.30	1.21E+41	1964.186	819.3	18.40	1.75E+40
1961.707	-86.2	14.02	9.86E+41	1962.172	83.6	16.50	1.00E+41	1964.534	946.4	18.15	2.20E+40
1961.708	-85.8	14.10	9.16E+41	1962.184	88.0	16.70	8.36E+40	1964.610	974.1	18.15	2.20E+40
1961.710	-85.1	14.00	1.00E+42	1962.241	108.8	16.70	8.36E+40	1964.625	979.6	17.70	3.33E+40
1961.712	-84.4	14.06	9.51E+41	1962.518	210.0	16.70	8.36E+40	1964.682	1000.4	17.60	3.65E+40
1961.715	-83.3	13.86	1.14E+42	1962.564	226.8	16.70	8.36E+40	1964.710	1010.6	17.70	3.33E+40
1961.718	-82.2	14.04	9.68E+41	1962.567	227.9	16.69	8.43E+40	1964.745	1023.4	17.90	2.77E+40
1961.721	-81.1	13.90	1.10E+42	1962.580	232.7	16.68	8.51E+40	1964.786	1038.4	17.90	2.77E+40
1961.750	-70.5	14.08	9.33E+41	1962.600	240.0	16.70	8.36E+40	1964.868	1068.4	17.70	3.33E+40
1961.770	-63.2	14.05	9.59E+41	1962.650	258.2	16.70	8.36E+40	1964.901	1080.4	18.00	2.52E+40
1961.773	-62.1	14.10	9.16E+41	1962.660	261.9	16.80	7.62E+40	1964.902	1080.8	18.00	2.52E+40
1961.775	-61.4	14.00	1.00E+42	1962.665	263.7	16.72	8.20E+40	1964.915	1085.5	17.90	2.77E+40
1961.776	-61.0	13.80	1.21E+42	1962.671	265.9	16.80	7.62E+40	1964.975	1107.4	18.10	2.30E+40
1961.786	-57.3	14.00	1.00E+42	1962.682	269.9	16.70	8.36E+40	1965.016	1122.4	18.10	2.30E+40
1961.825	-43.1	13.86	1.14E+42	1962.683	270.3	16.74	8.05E+40	1965.156	1173.5	18.90	1.10E+40
1961.827	-42.4	14.25	7.98E+41	1962.726	286.0	16.90	6.95E+40	1965.175	1180.5	18.50	1.59E+40
1961.828	-42.0	14.30	7.62E+41	1962.742	291.8	17.15	5.52E+40	1965.178	1181.6	18.10	2.30E+40
1961.829	-41.6	14.40	6.95E+41	1962.748	294.0	17.30	4.81E+40	1965.569	1324.4	18.40	1.75E+40
1961.830	-41.3	14.30	7.62E+41	1962.750	294.8	16.98	6.46E+40	1965.600	1335.7	18.40	1.75E+40
1961.838	-38.4	14.10	9.16E+41	1962.751	295.1	17.15	5.52E+40	1965.732	1383.9	18.40	1.75E+40
1961.847	-35.1	14.20	8.36E+41	1962.759	298.0	17.20	5.27E+40	1965.759	1393.8	18.40	1.75E+40
1961.852	-33.2	14.00	1.00E+42	1962.775	303.9	17.38	4.47E+40	1968.729	2478.6	21.20	1.32E+39
1961.863	-29.2	13.70	1.32E+42	1962.805	314.8	17.50	4.00E+40	1968.805	2506.3	21.00	1.59E+39

NOTE. — The integrated emission during the 970 days from date 1961.539 to 1964.186 is  $2.4 \times 10^{49}$  erg

ing length convection was left on in the remaining core during the interpulse periods, but not in the presence of shocks or in the ejecta.

To keep the number of parameters manageable, only two choices of initial carbon abundance were used, with the values determined by a variable  $3\alpha$  rate. One, nominally the “low carbon” case, used the same reaction rates

as (Woosley 2017), which corresponds to a choice of  $f_{3\alpha} = 1$ ,  $f_{\text{Buch}} = 1.2$  in Table 1 of Woosley & Heger (2021). Another, the “high-carbon” case, used  $f_{3\alpha} = 1.5$  and  $f_{\text{Buch}} = 1.2$ , that is, the  $3\alpha$ , and only the  $3\alpha$  rate was increased. This had the effect of approximately doubling the carbon mass fraction after helium burning and gives results similar to the “1/1.35” case in Table 1 of Woosley

& Heger (2021). As we shall see, this larger carbon abundance has the effect of increasing the helium core masses required for a given duration of pulsing activity by about 20% and generally weakening the explosion. The range explored probably spans the experimentally expected error bars for the  $^{12}\text{C}(\alpha, \gamma)^{16}\text{O}$  and  $3\alpha$  reaction rates.

Also important and uncertain is the treatment of convection in the hydrogen envelope of the progenitor star. Red and blue supergiant envelopes with the same mass atop of the same helium and heavy element core will have different interactions when traversed by a shock wave. Stars with smaller radii will, initially at least, give fainter SNe. SN 1987A is the most familiar example of this. Unfortunately, convection in the envelopes of very massive, radiation-dominated stars is not well understood. Crudely, the convection is represented using “mixing length” theory, where the characteristic length for convective energy dissipation is some factor,  $\alpha$ , times the pressure scale height. Semiconvection, convective overshoot mixing, convective dredge up, and rotational mixing are additional complications. Historically, KEPLER has used a mixing length parameter,  $\alpha = 1$ . With modern opacities and this value of  $\alpha$ , KEPLER has tended to give SNe II-P progenitors with radii that were too large by about a factor of two compared with what was needed to properly replicate the light curve (Dessart & Hillier 2011; Dessart et al. 2013). As those authors noted, increasing  $\alpha$  to 2 or 3 reduced the pre-SN radius by the necessary amount (see also Paxton et al. 2018). A smaller radius during helium burning would also help to bring KEPLER models into better agreement with those of the Geneva group (e.g., Schaerer et al. 1993). Additionally, recent three-dimensional simulations (Goldberg et al. 2021) have confirmed that, for red supergiant envelopes, a value of  $\alpha$  of 2 or 3 is a better choice, at least in the MESA code. We thus explored two sets of models with larger  $\alpha$ , as well as our more traditional case of  $\alpha = 1$ .

Surface boundary conditions also matter. Sanyal et al. (2015) have discussed the radius inflation, up to a factor of 40, that occurs in their models for stars with main sequence mass over  $40 M_{\odot}$ . The fact that the luminosity is effectively super-Eddington in regions with high opacity near the surface leads to convection, pulsations, radius expansion, and density inversions. The authors speculated that the instabilities they observed might be related to luminous blue variables (see also Jiang et al. 2018). We see the same effects in our models here, all of which are over  $90 M_{\odot}$ . With the customary low surface boundary pressure ( $P_{\text{bound}} = 100 \text{ dyne cm}^{-2}$ ), pre-SN radii exceeding  $1.5 \times 10^{14} \text{ cm}$  are common as well as density inversions of up to an order of magnitude in the outer solar mass.

Sanyal et al. (2015) do not specify what the actual radius should be. It is probably variable, but the absence of observed red supergiants with very high mass, and the association of some SNe II<sub>n</sub> with LBV-like progenitors (Smith 2014) suggests the probability of smaller radii. To explore this possibility, we used a greatly increased surface boundary pressure,  $5000 \text{ dyne cm}^{-2}$ , in a subset of models to at least partly suppress radius expansion. This is a problem worth further investigation, but for now the goal is just to bracket the expected radii of SN 1961V

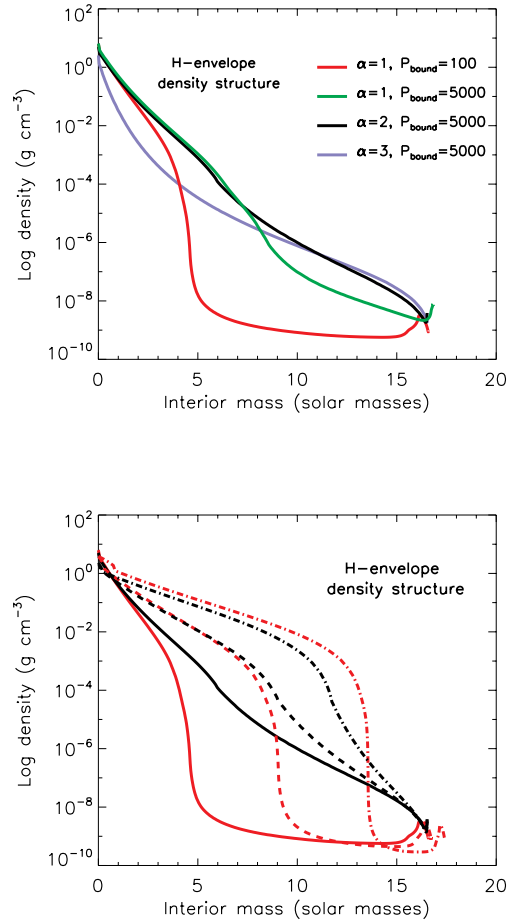


FIG. 1.— Density structure of the hydrogen-rich envelope of several models with nearly the same final helium core and envelope masses. (top:) The structure is evaluated at the onset of pulsational activity ( $T_c = 1.2 \text{ GK}$ ) for four models with helium core masses (not plotted) near  $46.5 M_{\odot}$  and hydrogen envelopes near  $17 M_{\odot}$ , but different values of mixing length parameters ( $\alpha$ ) and surface boundary pressures ( $P_{\text{bound}}$ ). Zero on the mass scale is the base of the hydrogen envelope. The models are TH102p25, TH102p45\*, M105p6, and M106p75 in Table 3. Higher surface boundary pressure and greater mixing lengths lead to denser, more compact envelopes with smaller radii. (bottom:) The density structure for Models TH102p25 (red lines,  $\alpha = 1, P_{\text{bound}} = 100 \text{ dyne cm}^{-2}$ ) and M105p6 (black lines,  $\alpha = 2, P_{\text{bound}} = 5000 \text{ dyne cm}^{-2}$ ) evolve considerably following helium depletion (dash-dotted lines) and pre-carbon ignition ( $T_c = 0.5 \text{ GK}$ ; dashed lines). The solid lines show the structure at carbon depletion ( $T_c = 1.2 \text{ GK}$ ) as in the top frame. In these two models, a surface convection zone eats deeper into the envelope as the core contracts moving more matter to larger radii. Note surface density inversions in Model TH102p25.

progenitors, even if the physics is not well understood.

To illustrate the sensitivity, four models were calculated that were constrained, by varying initial mass and mass-loss rate, to give approximately the same final helium core and hydrogen envelope masses. These models used different overshoot parameters  $\alpha = 1, 2, \text{ and } 3$ , and surface boundary pressures. These are models TH102p25, TH102p45\*, M105p6, and M106p75 in Table 3. Fig. 1 shows the hydrogen envelope structure late in

their evolution. The dominant effect comes from increasing the surface boundary pressure, which has the effect of suppressing the low temperature, high opacity regions near the surface. This helps alleviate the density inversion and leads to a more compact structure. The mixing length also has an important secondary effect, larger values making the envelope more compact.

Fig. 1 (bottom panel) also shows that, for at least two of these models, TH102p25 and M105p6, much of the difference in pre-SN structure develops after helium depletion ( $Y_c < 0.01$ ) as a deep surface convective zone eats into the envelope. This is a brief period in the life of the star. From helium depletion to explosion is only about 10,000 years, and from  $T_c = 0.5$  GK to explosion it is 1600 years. Unless the SN progenitor itself is observed, observers are unlikely to catch a star during this phase of its life, but the changes are significant for the pre-SN structure.

Fortunately, since we are only interested in the main light curve and not shock break out, the initial radius of the star doesn't matter much except for the first pulse, i.e., the beginning of long complex events and PISN. It also matters, to a lesser extent, for the early CSM interaction which depends on how much matter is accelerated to high velocity by shock break out. The first pulse ejects the residual hydrogen envelope and what happens afterward depends more on the energy of that first pulse and the waiting time until the next one than the initial radius. Shock break out in very massive Type II SNe like those studied by Kasen et al. (2011) may need reexamining.

### 3.2. The Allowed Mass Range

The properties of a Type II PPISN progenitor are chiefly determined by: a) the mass of its helium core; b) the mass fraction of carbon in that core at the time of central carbon ignition; and c) the mass and radius of its hydrogen envelope (see Table 2 and Table 3). The energy of the explosion, the duration of pulsing activity, and the intervals between pulses are all set by the helium core mass and carbon fraction. The light curve and spectrum are additionally sensitive to the hydrogen envelope mass and its structure. Secondary parameters are the metallicity, which affects the mass loss, opacity, and the strength of the hydrogen burning shell; the density profile within the hydrogen envelope, which also affects the light curve; the opacity itself, which affects the radius; and the treatment of convection in the model, both before and between the pulses. Neglecting rotation, as we do here, adds additional uncertainty as does the one-dimension treatment of the explosion hydrodynamics.

That said, any two stellar evolution calculations that give the same helium core mass, carbon mass fraction, and hydrogen envelope mass will produce qualitatively similar explosions. The initial mass, metallicity, and mass loss rate matter chiefly by affecting these three derived quantities.

Previous work on PPISNe allows us to narrow the range of He core masses and other parameters for the special case of SN 1961V. For the nuclear reaction rates and convection physics assumed in Woosley & Heger (2021), having pulses that last at least a few weeks in order to add structure to the  $\sim 150$  day light curve of SN 1961V, rules out pre-SN helium cores less massive than  $M_{\text{He}} \lesssim 40 M_{\odot}$  and zero age main sequence masses

less than  $M_{\text{ZAMS}} \lesssim 95 M_{\odot}$ , although this corresponding initial mass depends somewhat on the adopted mass-loss rates. If we look for explosions with pulsational activity comparable to the 200 day duration of SN 1961V, then core masses  $47 \pm 1 M_{\odot}$  ( $M_{\text{ZAMS}} \approx 100 M_{\odot}$ ) are preferred. See also Figs 15 - 17 of Woosley (2017). These choices are sensitive to the carbon abundance in the pre-SN star.

The largest helium core masses of interest are for cases where the pulsational activity goes on much longer than SN 1961V itself. One possibility (§ 5.2) is that only the first pulse or two make SN 1961V, but the star survives until much later, pulsing again just before dying, but perhaps not producing a bright optical display at that time. The gross upper limit for that case is then the boundary between pair instability and pulsational pair instability SN which is  $M_{\text{He}} \approx 65 M_{\odot}$  and  $M_{\text{ZAMS}} \approx 140 M_{\odot}$  for the low carbon case and  $M_{\text{He}} \approx 70 M_{\odot}$  and  $M_{\text{ZAMS}} \approx 150 M_{\odot}$  for the high-carbon case. Most of these very high mass stars will have initial flashes that are too energetic for SN 1961V. In practice, it turns out that mass limits only about 20% greater than for the single event model are appropriate. Even given the uncertainty in carbon abundance, the helium core mass for all successful PPISN models for SN 1961V is probably between 45 and 55  $M_{\odot}$ , corresponding to a zero age main sequence mass between 100 and 130  $M_{\odot}$ . If one includes the unlikely PISN models of § 4, these limits are raised to 75  $M_{\odot}$  and 160  $M_{\odot}$  respectively, but these models are unlikely explanations.

Knowing the pre-SN helium core mass tightly constrains the pre-SN luminosity of the star and the energetics of the explosion. In KEPLER, the luminosity at the onset of carbon burning for stars with helium cores in the mass range 45 to 55  $M_{\odot}$  is limited to 1 to  $1.3 \times 10^{40}$  erg  $\text{s}^{-1}$ . In some cases, the luminosity actually decreases slightly just prior to explosion in response to the contracting core, so these are upper limits. We shall find that the total kinetic energy of the explosion for stars in this mass range is near  $7 \times 10^{50}$  erg for the low carbon case and  $4 \times 10^{50}$  erg for the high-carbon case. Most of the mass ejected is residual helium-hydrogen envelope, which could in principle range from 0 to  $(M_{\text{ZAMS}} - M_{\text{He}}) \approx 50 M_{\odot}$ . Very small and large values are unlikely though since mass loss is not negligible for a reasonable choice of metallicity, and a long plateau is not possible with too little envelope. Taking  $M_{\text{ej}} \approx 10 - 15 M_{\odot}$  as representative of the ejected mass, a typical velocity is then  $(2E_{\text{exp}}/M_{\text{ej}})^{1/2} \approx 1600 - 2600$  km  $\text{s}^{-1}$ , though one expects variation with higher velocities near the outer edge and lower ones deep inside. That this ballpark number agrees with what is observed at late times for the speed of the bulk of the SN 1961V ejecta (Branch & Greenstein 1971) is encouraging.

These estimates suggest a focus on models with masses  $M_{\text{ZAMS}} \approx 95$  to  $115 M_{\odot}$  for the low carbon case and  $M_{\text{ZAMS}} \approx 115$  to  $135 M_{\odot}$  for the high-carbon case. A few more massive cases were considered in § 4. A metallicity of 1/3 solar was chosen for all models, consistent with estimates for the vicinity of SN 1961V, and the mass-loss rate was adjusted to give approximately desired envelope mass. Again, somewhat lower mass-loss rates (i.e. even lower than just scaling standard rates for metallicity) are justified due to recent downward revisions in stellar wind mass-loss rate prescriptions (Smith 2014). In general,

the successful explosions had lost most of their hydrogen envelope, but still retained an appreciable amount.

The mass ranges and envelope masses motivated by these considerations then define the models selected for study (Table 2 and Table 3). The models are named according to the choices of initial mass, mass-loss rate, mixing length parameter, and boundary pressure. Not all combinations were explored. All models used the same one-third solar metallicity composition. The “TH” models (here “TH” is for third solar metallicity to distinguish them from the “T”, tenth solar metallicity models, of Woosley 2017), had  $\alpha = 1$  and  $P_{\text{bound}} = 100 \text{ dyne cm}^{-2}$ . The “M” models (“M” is for “mixing length”) used a mixing length parameter  $\alpha = 3$  and a boundary pressure of  $5000 \text{ dyne cm}^{-2}$ . The “A” models used a mixing length parameter  $\alpha = 2$ , a boundary pressure of  $5000 \text{ dyne cm}^{-2}$ , and a large  $3\alpha$  rate as described above so as to give a high carbon abundance after helium burning. Models were further named for their initial mass and mass-loss rate reduction, e.g., Model T102p25 had an initial mass of  $102 M_{\odot}$  and a mass-loss rate 25% of the standard value. Sometimes the “p $\alpha$ ” subscript is dropped in the plots where no ambiguity arises, e.g., most of the TH models used p25 for mass loss.

### 3.3. Presupernova Evolution

The stars here all lived approximately 2.7 million years as bright, hot main sequence stars with effective temperatures near  $50,000 \text{ K}$  and luminosities  $0.6 (90 M_{\odot})$  to  $1.0 (140 M_{\odot}) \times 10^{40} \text{ erg s}^{-1}$ . This was followed by approximately 300,000 years as helium burning giant stars with luminosities from  $0.8$  to  $1.4 \times 10^{40} \text{ erg s}^{-1}$ . The main sequence evolution is straightforward and has been studied many times (e.g. Schaerer et al. 1993). The radius during helium burning is less certain and dependent on convection and surface boundary pressure (§ 3.1). For  $\alpha = 1$ , the models all developed deep surface convection zones at the end characterized by large radii and density inversions. That is they experienced radius inflation and became cool supergiants. Halfway through helium burning, typical effective temperatures were  $\approx 4500 \text{ K}$ .

For models with  $\alpha = 2$  or  $3$  and high surface pressures, the luminosities were nearly the same, but the radii were smaller by a factor of a few. Effective temperatures were thus  $7500$  to  $8500 \text{ K}$ . In this case, both as helium burning stars and SN progenitors, the stars would most likely have appeared as F-supergiants (see also Goodrich et al. 1989) with a relatively small bolometric correction. This is consistent with expectations for eruptive LBV-like stars (Smith et al. 2004).

Since the progenitor of SN 1961V was repeatedly observed starting in 1937 (Table 1), the last 25 years of the models’ lives are of special interest. During this time, all models were contracting from carbon ignition at about  $0.75 \text{ GK}$  to pair instability when oxygen ignited around  $\text{GK}$ . Most of the star’s luminosity during this time, both in photons and neutrinos was derived from this contraction and not nuclear fusion. Unlike lower mass SNe, there is no extended period of carbon (centuries) or oxygen (months) burning. During this contraction, no convection occurred inside the helium core until the last week. Thus there was very limited time for acoustic transport to the surface of a large energy flux that might drive mass loss (Shiode & Quataert 2014). In the last few months,

the hydrogen burning shell was super-heated by the contraction of the helium core and generated a power that, were it communicated to the surface, would have been super-Eddington, but there was insufficient time even for convection to do so. The star expanded slightly in response. The star thus often died in a state of thermal disequilibrium with the power emerging from the helium core exceeding what was being emitted from the surface.

## 4. PAIR-INSTABILITY MODELS

Stars with initial mass above  $80 M_{\odot}$ , the (smallest) lower limit on progenitor mass imposed on SN 1961V by Kochanek et al. (2011), are not expected to explode by neutrino transport or to leave a neutron star (e.g. Heger & Woosley 2002; Sukhbold et al. 2016; Rahman et al. 2021). They either blow up completely as pair-instability supernovae (PISN), leave black hole remnants following an epoch of violent nuclear-fueled pulsations (PPISNe), or collapse directly to black holes without mass ejection or bright transient emission.

A PISN explanation is possible for SN 1961V, but not very likely. Models with bolometric light curves having the same approximate duration and luminosity as the major event of SN 1961V have been published. See Model R150 and Fig. 8 of Kasen et al. (2011) and Models P150 and P175 and Fig. 13 of Gilmer et al. (2017). If the entire star explodes in one pulse though, a very oxygen-rich SN remnant would result that doesn’t seem to have been observed (Goodrich et al. 1989). The total kinetic energy of the event would exceed  $4 \times 10^{51} \text{ erg}$ , and much of the hydrogen-rich ejecta would move faster than  $2000 \text{ km s}^{-1}$ , even if the envelope were massive. A PISN model, by itself, would also leave unexplained the brightening to  $m_{\text{pg}} = 15.8 \text{ mag}$  observed one year prior to the peak of the SN (Table 1) and the years of emission after the peak. We shall find PPISN models that fit SN 1961V better, and expect them to be more common in nature. Still, PISN models are worth brief exploration, if only to provide some interesting limits on the pre-SN mass and luminosity.

Six PISN models (Table 2) were calculated that had the approximate duration of SN 1961V. Each had a main sequence mass of  $140 M_{\odot}$  or more, a metallicity one-third solar, and a mass-loss rate well below standard values expected for this metallicity. Compared with Kasen et al. (2011) and Gilmer et al. (2017), these models have the advantage of a more realistic metallicity for SN 1961V,  $1/3 Z_{\odot}$  vs  $10^{-4} Z_{\odot}$ , and possibly a more realistic radius, but they have the disadvantage of using KEPLER to calculate their light curves rather than the more capable transport codes SEDONA or STELLA. KEPLER should be capable of providing approximate bolometric light curves though. The pre-SN luminosities and radii in Table 2 were evaluated at carbon depletion, just a few weeks before pulsations commenced, and are representative pre-SN properties. They evolve very little during the last century of the star’s life. More massive models than in Table 2 would have been even more energetic ( $\approx 10^{52} \text{ erg}$ ), produced brighter light curves, and larger amounts of  $^{56}\text{Ni}$  ( $> 0.1 M_{\odot}$ ). The hydrogen envelope, even in the absence of any mass loss, would move much faster than  $2000 \text{ km s}^{-1}$ , and the  $^{56}\text{Ni}$  mass would exceed  $0.2 M_{\odot}$  producing very bright tails on the light curves. These traits are incompatible with observation, and we



TABLE 2. SINGLE PULSE PAIR-INSTABILITY SUPERNOVA MODELS

Mass ( $M_{\odot}$ )	Mass Loss Multiplier	$\alpha$	$M_{\text{He}}$ ( $M_{\odot}$ )	$X(^{12}\text{C})$	$M_{\text{preSN}}$ ( $M_{\odot}$ )	$R_{\text{preSN}}$ ( $10^{13}$ cm)	$L_{\text{preSN}}$ ( $10^{40}$ erg s $^{-1}$ )	$M_{\text{Ni}}$ ( $M_{\odot}$ )	$\text{KE}_{\text{eject}}$ ( $10^{50}$ erg)	$E_{\text{rad}}$ ( $10^{50}$ erg)
TH140p0	0	1	68.05	0.0791	139.95	22	1.3	0.0280	45.4	2.41
TH140p125	.125	1	67.36	0.0675	104.27	23	1.3	0.0450	54.8	1.95
M140p25	.25	2	66.53	0.0795	107.05	7.5	1.2	0.0148	37.4	0.43
M140p125	.125	2	66.81	0.0776	123.99	7.1	1.3	0.0316	47.6	0.46
A155p2	.20	2	74.96	0.126	127.07	6.9	1.4	0.0102	57.1	0.48
A160p2	.20	2	77.18	0.127	129.92	7.4	1.4	0.204	149	1.20

NOTE. — The mass loss multiplier is applied in addition to the usual reduction for metallicity,  $Z^{1/2}$ .

conclude that the progenitor of SN 1961V must have had a bolometric luminosity less than  $1.4 \times 10^{40}$  erg s $^{-1}$  and an initial main-sequence mass less than  $160 M_{\odot}$ , even if it was a PISN.

Unlike the pre-SN luminosity, the PISN light curves are sensitive to the radius and structure of the envelope (§ 3.1, Fig. 2). Four models, M140p25, M140p125, A155p2, and A160p2 employed a higher surface boundary pressure and larger mixing length multiplier, and thus had reduced progenitor radii. Effective temperatures for the pre-SN stars were 7500 - 8500 K for M140p25, M140p125, A155p2 and A160p2 and 4500 K for TH140p125 and TH140p0. Typically the BSG progenitor radius was about three times smaller than for the red supergiant models, TH140p0 and TH140p125 (Table 2). This resulted in light curves that were briefer and less luminous. In addition, Models A155p2 and A160p2 used reaction rates that favored a larger carbon abundance after helium burning and were thus weaker explosions.

All PISN models produced small, but consequential amounts of  $^{56}\text{Ni}$  (Table 2). The  $^{56}\text{Ni}$  mass is sensitive to the temperature reached in the pulse and hence to the mass of the helium core and carbon mass fraction. It would be larger for more massive helium cores or less carbon in the pre-SN star. Model A160p2 is an upper limit where even the luminosity on the tail of SN 1961V is overproduced by radioactivity. The other models have durations, hydrogen velocities, and luminosities crudely in agreement with SN 1961V, but with substantial disparities. The red giant models are too bright, owing to their large initial radii and high explosion energy, and can be ruled out. The bluer models are still too bright and too brief, though the latter could partly be an artifact of using KEPLER with just electron scattering opacity plus an additive constant. A recalculation of Model R150 of Kasen et al. (2011) using just KEPLER gave a shorter plateau, so this may be an issue worth revisiting.

But none of the light curves in Fig. 2 show the late time brightening observed when SN 1961V reached its peak, and they all require relatively low mass-loss rates for a metallicity of  $1/3$  solar in order to preserve a large mass of hydrogen envelope. The models do not explain the pre-explosive brightening one year before the observed peak (Table 1), though this could be some sort of pre-SN LBV outburst (Goodrich et al. 1989). They also do not explain the enduring emission seen for at least three years after the peak, though circumstellar interaction could be invoked (Smith et al. 2011). The models predict a large mass of oxygen (roughly  $45 M_{\odot}$ ) and silicon (roughly  $5$

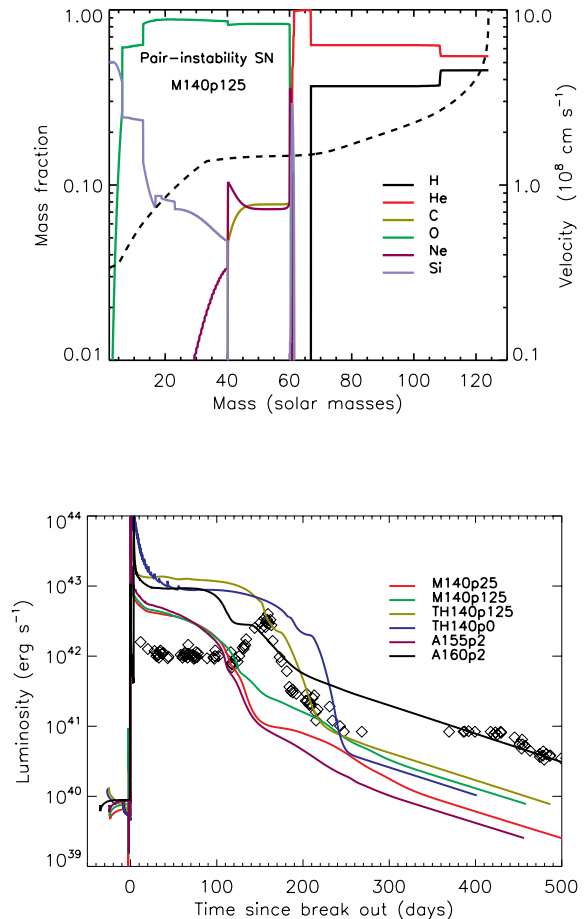


FIG. 2.— (top:) Ejected composition and terminal velocity for Model M140p125 and (bottom:) approximate bolometric light curves for the six PISN models in Table 2. The velocity and composition of Model M140p125 are typical of the five models that have some similarity to SN 1961V, although the hydrogenic velocity is slower for Model TH140p0 which had no pre-SN wind mass loss. Models M140p25, M140p125, A155p2, and A160p2 were blue supergiants and had a more compact structure when they exploded. Models TH140p0 and TH140p125 were red supergiants with very low density hydrogen envelopes. Tails due to the decay of  $^{56}\text{Co}$  are apparent. None of the models resembles closely the observations of SN 1961V, which is why we favor pulsational pair models for SN 1961V as opposed to a true PISN.



$M_{\odot}$ ) moving at very slow speed,  $\sim 1000 \text{ km s}^{-1}$  (Fig. 2). Given the low level of radioactivity, perhaps these very large masses might be difficult to detect, but by now they cover a region roughly  $0.1 \text{ pc}$  in radius.

A PISN model is thus not completely ruled out for SN 1961V, but there are PPISN models that look more promising and should occur more frequently

### 5. PULSATONAL PAIR-INSTABILITY MODELS

There are three subclasses of PPISN models that could plausibly explain SN 1961V. In the first (§ 5.1), the principle outburst of SN 1961v was a single SN-like event consisting of multiple pulses followed soon afterward by a final collapse to a black hole that occurred while most of the ejecta was still optically thick. Most of the pulses occurred early on, but the light curve continued to accumulate energy well after core collapse. This model at least has the advantage of providing a credible explosion mechanism for a very massive progenitor, but other activity prior to or long after the main event in 1961 must be attributed to variability of the pre-SN star (before explosion) and shock interaction with the star’s wind (after the explosion).

In the second case (§ 5.2), SN 1961V itself resulted from one or two initial pulses, but those pulses were part of a continuing multiplet that resumed, after a long dormant period, decades or even centuries later. This is the only scenario where anything resembling a normal star, could still occupy the site of SN 1961V several years later. Powered by Kelvin-Helmholtz contraction, not nuclear burning, and perhaps supplemented by accretion from fallback, the star’s luminosity would remain near Eddington. That is, it would be close to its pre-explosive value. The star could still be there or it could be gone by now, replaced by a black hole of about  $45 M_{\odot}$ .

The third case (§ 5.3) assumes that SN 1961V underwent a series of explosions lasting several years. The core has long since collapsed to a black hole, but only after multiple shell ejections and SN-like outbursts. The best fit to the onset of SN 1961V in this case is obtained not by fitting the onset of the SN to the first pulse, but to the second or third pulse happening hundreds of days later. In this scenario, bright events prior to SN 1961V itself must somehow have been missed by observers at the time. Because the colliding shells are not very geometrically thick and the optical depth is low, rapid temporal variation is possible, but collisions at very late time might have low optical efficiency. The energy that is radiated is given by the differential speed of colliding shells, which may be much less than their bulk spectroscopic speeds.

For a given carbon mass fraction, these three possibilities correspond to narrow ranges of helium core mass. For the “TH” models in Table 3 the appropriate ranges for the three outcomes are  $46 - 48 M_{\odot}$ ,  $50 - 52 M_{\odot}$ , and  $48 - 50 M_{\odot}$ . No matter which subclass or carbon abundance is invoked, the total mass of the pre-SN star is constrained to be approximately  $65 \pm 5 M_{\odot}$  and a black hole of about  $45 \pm 5 M_{\odot}$  is the final remnant. The more massive black holes in this range are favored by a large carbon abundance.

#### 5.1. Single Events

For relatively low-mass helium cores, pulsational activity is confined to the first 100 days (Woosley 2017).

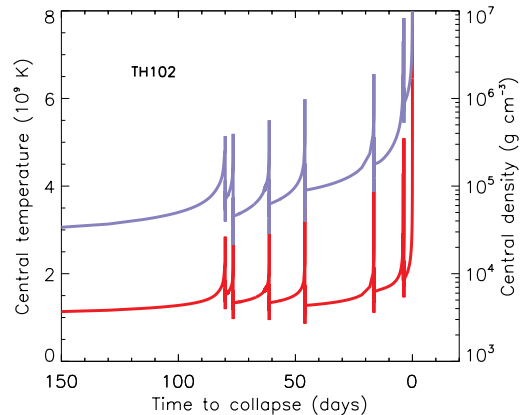


FIG. 3.— Pulsing history of Model TH102p25, a representative example of the class of single event models. The central temperature and density are shown as a function of time to core collapse. Six well defined pulses happen in a space of 80 days. The last rise to a central temperature above 8 GK indicates collapse to a black hole. No outward shock is generated by this final event.

“Single events” here really means a rapid succession of pulses that are grouped closely together while the SN is still optically thick (e.g. Fig. 3), producing a single observed bright SN, albeit with a structured light curve. Depending on the timing and energies of these pulses, collisions between ejected shells may continue well after the black hole forms, but these collisions do not persist to sufficiently late times to explain the many years that SN 1961V maintained a luminosity in excess of  $10^{40} \text{ erg s}^{-1}$ .

Fig. 4 shows the light curves for six “TH” models and five “M” models in Table 3 with total pulsational durations less than 120 days (Fig. 3). The “TH” models have identical physics to Woosley (2017) and “low carbon” abundances, i.e., a relatively high rate for  $^{12}\text{C}(\alpha, \gamma)^{16}\text{O}$  and low rate for  $3\alpha$  (Woosley & Heger 2021). The final ejecta velocities and effective emission temperatures are shown for these models in Fig. 5. Models less massive than TH95 are disallowed by their low velocities for envelope masses sufficient to maintain the continuity and duration of the light curve.

Four phases of the light curve can be distinguished: 1) A bright, brief, ultra-violet transient as the first shock breaks out; 2) A plateau as the shock heated envelope is ejected by the first pulse and recombines. This phase is fainter for models with smaller radii and longer for more massive models, but not more than a few weeks. It is the analogue of an ordinary Type II-P SN; 3) A series of broad peaks generated by multiple pulses interacting with optically thick matter ejected by previous pulses. The light diffuses ahead of the shock and causes a significant brightening as it approaches the photosphere, but each peak also has a “tail” that can be obscured by subsequent pulses except for the last; and 4) Narrow spikes resulting from the collision of geometrically thin shells. These shells are accumulations of matter generated by pile up at both the forward and reverse shocks associated with each pulse. The width of these spikes is underestimated and the peak luminosity overestimated in this 1D

TABLE 3. PULSATONAL PAIR-INSTABILITY MODELS

Mass ( $M_{\odot}$ )	Mass Loss Multiplier	$\alpha$	$M_{\text{He}}$ ( $M_{\odot}$ )	$X(^{12}\text{C})$	$M_{\text{preSN}}$ ( $M_{\odot}$ )	$R_{\text{PreSN}}$ ( $10^{14}$ cm)	$M_{\text{Fe}}$ ( $M_{\odot}$ )	Duration (days)	$M_{\text{final}}$ ( $M_{\odot}$ )	$\text{KE}_{\text{eject}}$ ( $10^{50}$ erg)	$E_{\text{rad}}^a$ ( $10^{50}$ erg)
TH93p25	.25	1	40.44	0.113	60.13	18	2.54	7.94	38.3	3.24	0.33
TH95p25	.25	1	42.68	0.109	60.49	18	3.23	20.5	39.4	5.26	0.53
TH97p25	.25	1	43.37	0.106	61.12	18	2.52	24.6	39.4	5.70	0.57
TH99p25	.25	1	44.79	0.100	61.59	18	2.86	44.2	40.0	6.27	0.82
TH99p125	.125	1	45.19	0.104	77.56	20	2.19	51.1	40.6	6.44	0.75
TH100p25	.25	1	45.50	0.0982	61.85	18	2.69	69.5	40.0	7.72	1.22
TH101p25	.25	1	45.60	0.100	62.43	18	2.52	61.8	40.2	7.53	1.15
TH102p25	.25	1	46.14	0.100	62.73	18	2.27	80.0	40.8	7.35	1.26
TH102p45 <sup>*b</sup>	.45	1	46.49	0.0991	62.93	7.9	2.71	56.3	42.1	8.35	0.89
TH102p125	.125	1	46.10	0.104	79.38	2.0	2.33	74.0	41.2	6.92	0.98
TH103p25	.25	1	46.68	0.0996	63.09	18	2.39	102	41.1	7.60	1.54
TH104p25	.25	1	47.01	0.0964	66.46	16	2.50	231	41.6	7.37	1.97
TH105p25	.25	1	48.84	0.0897	63.07	18	2.56	361	44.4	7.20	2.54
TH106p25	.25	1	47.34	0.0996	64.32	18	2.72	188	42.3	7.31	1.80
TH107p25	.25	1	50.03	0.0882	63.66	18	2.16	567	44.2	8.20	3.14
TH108p25	.25	1	49.71	0.0916	64.38	18	2.20	440	44.3	7.64	2.94
TH109p25	.25	1	50.05	0.0938	64.03	18	2.89	590	44.4	7.20	3.58
TH110p25	.25	1	50.49	0.0911	65.09	18	2.71	703	44.7	8.02	3.02
TH111p25	.25	1	51.36	0.0907	65.36	18	2.53	1050	46.9	7.04	3.92
TH112p25	.25	1	51.74	0.0907	65.80	18	2.14	1300	47.2	7.26	3.99
TH113p25	.25	1	51.32	0.0935	66.47	18	2.38	872	45.7	7.56	3.91
TH114p25	.25	1	51.63	0.0915	70.18	16	1.93	14600	46.1	8.33	1.35
TH115p25	.25	1	52.12	0.0901	70.51	16	1.99	39100	45.9	9.70	1.77
TH120p25	.25	1	54.56	0.0899	72.40	16	2.42	12900	48.7	11.5	0.51
M104p9	0.9	3	45.34	0.111	55.52	4.9	2.34	32.1	41.3	5.27	0.41
M105p9	0.9	3	45.55	0.109	55.56	4.9	2.58	37.9	41.2	5.39	0.46
M105p6	0.6	2	47.11	0.096	63.64	5.7	2.23	85.1	42.2	8.19	1.13
M106p9	0.9	3	46.14	0.110	55.83	4.9	2.50	40.2	41.6	5.71	0.48
M106p75	0.75	3	46.90	0.107	63.01	5.0	2.74	69.2	42.7	5.80	0.61
M107p9	0.9	3	46.72	0.104	55.67	4.9	2.46	78.4	41.8	5.31	0.69
M108p85	.85	3	47.53	0.108	58.44	5.0	2.66	83.1	42.6	6.32	0.86
M109p85	.85	3	48.05	0.107	58.55	5.0	2.68	110	43.8	5.75	0.85
M110p85	.85	3	48.53	0.106	58.61	5.0	2.27	160	43.9	5.83	1.10
A119p70	.70	2	53.01	0.174	61.49	6.7	2.38	19.8	49.7	4.17	0.27
A120p70	.70	2	53.75	0.172	60.57	6.7	2.40	29.7	50.4	4.34	0.37
A122p65	.65	2	54.99	0.172	65.01	6.8	2.20	50.7	50.7	4.24	0.43
A123p65	.65	2	55.15	0.172	65.15	6.9	2.39	149	51.2	4.15	0.73
A124p65	.65	2	55.73	0.171	65.02	6.9	2.15	257	51.3	4.23	0.74
A122p70	.70	2	54.87	0.173	60.92	6.6	2.13	115	50.1	4.14	0.57
A123p70	.70	2	55.01	0.171	61.20	6.5	2.17	135	51.0	3.90	0.67
A124p70	.70	2	55.48	0.167	60.91	6.5	2.17	258	51.1	3.86	1.08
A122p75	.75	2	55.14	0.158	57.48	5.3	2.05	683	50.8	3.29	0.68
A123p75	.75	2	54.94	0.169	57.40	5.3	2.33	192	51.1	3.07	0.74
A124p75	.75	2	55.08	0.165	57.48	5.4	2.08	306	50.2	3.48	0.82
A125p65	.65	2	56.30	0.171	65.64	6.8	2.32	221	52.6	3.98	1.00
A126p65	.65	2	56.54	0.168	65.48	6.8	2.23	382	51.7	4.01	1.22

NOTE. — <sup>a</sup> The radiated energy,  $E_{\text{rad}}$ , only includes the emission during the first 1000 days of pulsing activity.

<sup>b</sup> Model TH102p45 and all the “M” and “A” models had a surface boundary pressure of 5000 dyne  $\text{cm}^{-2}$ . The rest of the TH models had a boundary pressure of 100 dyne  $\text{cm}^{-2}$ .

study.

The durations in Table 3, which give the time between the launching of the first pulse and iron core collapse, are only approximations to the duration of the light curve. They can be overestimates of the observed light curve duration, since it takes up to two weeks for the first shock to traverse the envelope, and the final collapse produces no outgoing shock. For example, the time between first shock break out ( $t = 0$  in Fig. 4) and the launch of the final outgoing shock in Model TH102p25 is only 64 days, whereas the “duration” in Table 3 is 80 days. On the other hand, light can continue to diffuse out and shells continue to collide long after the core has collapsed and that lengthens the duration. The “M” models differ from

the “TH” models in having a higher surface boundary pressure and greater mixing length parameter. The resulting small radius leads to a light curve that is initially fainter, but not qualitatively different after the first two weeks.

The duration and luminosity of some of the models in Fig. 4, especially TH102p25 and M108p85, are in reasonable agreement with the observations of SN 1961V. There is also time variability due to repeated pulses, and a tendency of the luminosity to rise at late times as the pulses themselves become more violent. The heavier models, TH102p25 and TH103p25, also show “tails” resulting from continuing shock interaction after core collapse. It is important to recognize that no  $^{56}\text{Ni}$  is ejected in any

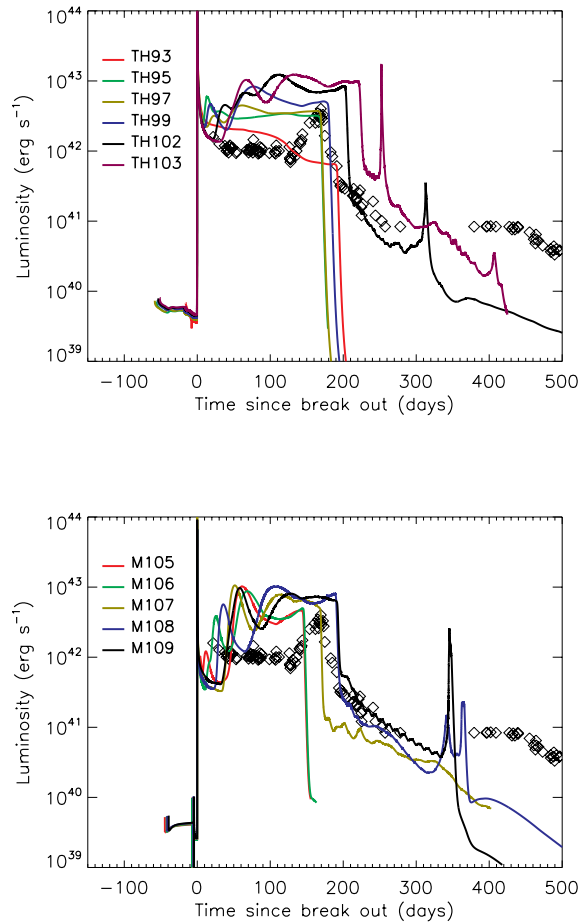


FIG. 4.— (top:) Bolometric light curves of Models TH93p25, TH95p25, TH97p25, TH99p25, TH102p25, and TH103p25 (Table 3). In all cases, the duration of pulsing activity is shorter than that of the initial plateau in the light curve. Multiple shocks from the pulses deposit energy in the deep interior that diffuses, in waves, to the photosphere. The greater the mass of the star the longer this pulsing persists. Later sharp structure in some of the light curve is introduced by fast moving thin shells that eventually catch up with slower ones after core collapse. (bottom:) Light curves for a similar set of models, M105p9, M106p9, M107p9, M108p85, and M109p85, with smaller radii and denser hydrogen envelopes. The initial masses are smaller because of the reduced mass-loss rates associated with the smaller radii. The light curves are similar to those for the “TH” models, except at early times when the smaller radius causes the emission to be fainter.

of these models; all of the observed luminosity is from diffusion out of shock-heated ejecta or CSM interaction. Still heavier models seem to be active too long, though see § 5.2 and § 5.3.

The shape of the light curve after the final brightest peak on the plateau is not well calculated in some of the models, especially the narrow spikes at 250 days in Model TH103p25 and 300 days in Model TH102C, and the ledges at the end of the plateau just before abrupt plunges by an order of magnitude in luminosity. The narrow spikes are artifacts of a crude treatment of radiation transport and shock hydrodynamics in a 1D model. As we shall see repeatedly, when the shock snowplows in a region of decreasing  $\rho r^3$ , with  $\rho$  the density and  $r$  the

radius, matter piles up in a geometrically thin shell, all moving at the same speed. In a multidimensional calculation this pile up is not nearly so extreme (Chevalier 1982; Chen et al. 2016) and the medium fragments into a clumpy shell with a thickness more comparable to 10 - 20% of its radius. As it is in 1D, when two very thin shells collide, the inelastic collision results in a discontinuous burst of energy as all their differential kinetic energy is abruptly converted to light. Brief spikes like the one in the late time light curve of TH103p25 should thus really be much broader and fainter. Thus, the absence of such narrow luminosity spikes in the observed light curve is not really in contradiction with these models. Similarly, the very sharp ledge of late time luminosity might be a numerical artifact. It comes from energy that has been radiated into the interior by a shock diffusing out again. The inward and outward transport of this radiation is not handled well in a Lagrangian code with a fixed inner boundary when the interior of the star has, in fact, already collapsed to a black hole. We suspect this late time plateau in luminosity is an overestimate, but a more realistic calculation is needed. With these adjustments, the agreement between observations and e.g., Model TH102p25 would improve at late times.

On closer inspection though, the “TH” and “M” models have problems. The ones with sufficient duration and velocity are just too bright, regardless of initial radius. The narrow width of the brightest observed peak is not reproduced, even if the questionable ledges of late time emission in the models are removed. The brightening a year before SN 1961V and multiple years of “afterglow” are not explained without invoking additional processes.

Better agreement can be achieved using the lower energy, high-carbon, A-series models, and a smaller radius for the pre-SN star. Fig. 6 shows the pulsing history and bolometric light curve of one such model, A123p65. This model has fewer, more widely spaced pulses than TH102p25, and the light curve thus shows less rapid variability. The smaller radius, by a factor of two, makes the initial display fainter, but most importantly, the larger carbon abundance weakens the pair instability. Overall, the kinetic energy of the explosion is reduced by almost a factor of two (Table 3) and, along with it, the total amount of radiant energy emitted by the SN. This brings the model light curves into much better agreement with SN 1961V. Model TH102p25 radiates  $1.26 \times 10^{50}$  erg while Model A123p65 radiates only  $7.3 \times 10^{49}$  erg, though this is still substantially more than observed for SN 1961V (Table 1) if no bolometric correction is assumed. The necessary helium core mass for instability is also raised from  $46.14 M_{\odot}$  to  $55.15 M_{\odot}$  and the main sequence mass goes from  $102 M_{\odot}$  to  $123 M_{\odot}$ . The black hole remnant mass increases from  $40.8 M_{\odot}$  to  $51.2 M_{\odot}$ .

Fig. 6 shows the velocity and local luminosity in Model A123p65 at several relevant times in its evolution. During the early plateau stage, not shown in Fig. 6, the photosphere lies in the outer ejecta where the speed is near  $2000 \text{ km s}^{-1}$ . During the brief period between core collapse and the beginning of the last major peak, the photosphere briefly recedes to lower velocity, although spectral lines would still be affected by the faster moving material farther out. With time, and especially near peak, the shock moves into higher velocity ejecta and eventually overtakes the photosphere. Brief spikes in the

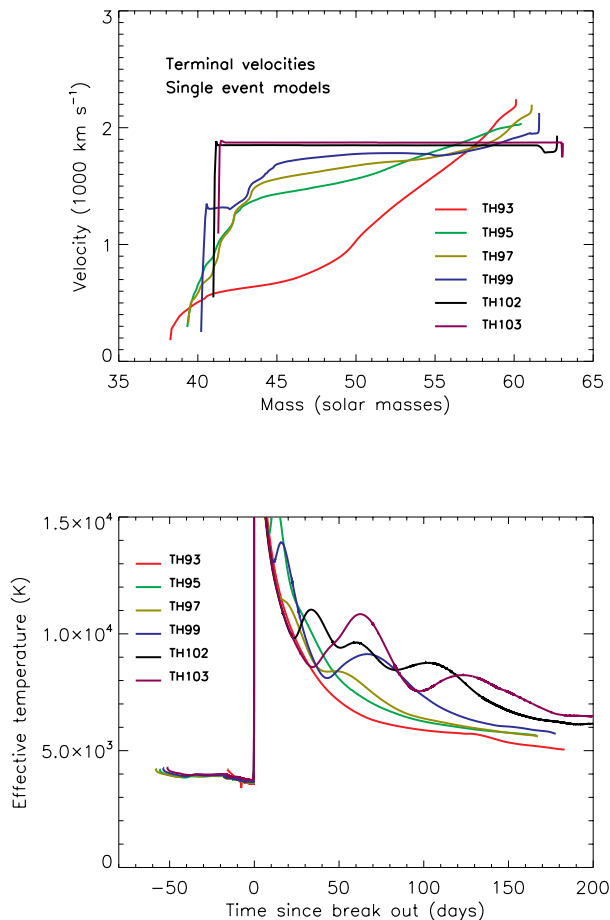


FIG. 5.— (top:) Terminal velocities and (bottom:) effective emission temperature histories of Models TH93p25, TH95p25, TH97p25, TH99p25, TH102C and TH103p25 during a time when the electron-scattering photosphere is well defined. Lower mass explosions resemble typical Type II-P SNe, albeit with a low energy to mass ratio. The higher mass models show distinctive signatures of pulsationally generated shock heating. At late times all the ejected matter ends up coasting at the same speed. This is an probably an artifact of the 1D calculation. During a pulse, the luminosity increases at nearly constant radius so the temperature rises.

light curve at 140 d and 200 d post-peak luminosity are due to colliding thin shells, the sharpness of which is overestimated in the 1D study.

The final velocities, after all shock interaction is over, are close to  $2000 \text{ km s}^{-1}$  (Fig. 5 and Fig. 7). TH102p25 had an envelope mass of  $16.6 M_{\odot}$ ; A123p65 had a lower-mass H envelope,  $10.0 M_{\odot}$ , but less kinetic energy. Testing the effect of a single parameter is difficult in these models because so many attributes are interconnected. For example, changing the envelope mass also changes the dynamics of the explosion and the pulse history. Changing the mass loss rate changes the envelope mass, but also the helium core mass. Decreasing the envelope mass of A123p65 would assist with narrowing the light curve at peak, but might also lead to longer gaps in the emission at earlier times.

While Model A123p65 is a phenomenal fit to the light

curve, it has some lingering issues. The model had velocity much greater than  $2000 \text{ km s}^{-1}$  in its interior close to the time of peak luminosity (Fig. 7), but this high speed was buried beneath optically thick material making Zwicky’s observation of  $3700 \text{ km s}^{-1}$  somewhat problematic. Both the brightening 366 days before peak and the subsequent years of enduring emission near the Eddington luminosity are unexplained. The pre-SN point on date 1960.942 might indicate activity as a LBV, as suggested by Goodrich et al. (1989), or some other phenomenon associated with the rapid Kelvin-Helmholtz contraction of the star following central carbon ignition and prior to oxygen burning. To be fair though, these issues would be vexing for any other explosion mechanism as well, and invoking such additional precursor variability and late-time CSM interaction is well justified, even if it is not uniquely predicted by the PPISN models.

It is certain, for example, that the very luminous progenitor star was rapidly shedding mass when it died. Reducing the hydrogen envelope to  $\sim 10 M_{\odot}$  during the 300,000 years that helium burned requires an average mass-loss rate greater than  $10^{-4} M_{\odot} \text{ y}^{-1}$ . This is easily achievable for the normal winds of luminous LBV-like stars (Smith & Owocki 2006), even without their eruptive mass ejection. Prodigious mass loss may also be assisted by close binary interaction, as is assumed to be the case for the precursor variability and mass loss before the eruption of Eta Carinae (Smith 2011; Smith et al. 2018). Given the necessity of some sort of surface activity to explain the brightening a year or more before explosion, and the superheating of the hydrogen burning shell by core contraction, the actual mass-loss rate was probably much larger near the end. Taking a representative value of  $0.001 M_{\odot} \text{ y}^{-1}$  and a wind speed of  $v_{\text{wind}} = 100 \text{ km s}^{-1}$ , plus a velocity for the outer few hundredths of a solar mass of ejecta of  $v_{\text{shock}} = 2500 \text{ km s}^{-1}$ , as the models find, implies a CSM interaction luminosity of  $L_{\text{CSM}} \approx 0.5 \dot{M} v_{\text{shock}}^3 / v_{\text{wind}} \sim 5 \times 10^{40} \text{ erg s}^{-1}$ , lasting for a year or so. The luminosity would gradually decline as the fastest moving ejecta were decelerated, or when the edge of the CSM shell was reached.

Altogether, we find that, if it is permissible to invoke precursor LBV-like variability to explain progenitor variations before SN 1961V and late-time CSM interaction (with dense CSM resulting from that same precursor variability) to explain the very late-time luminosity, then a PPISN model can do an excellent job of matching the very unusual main light curve, low observed expansion speeds, and low kinetic energy of SN 1961V.

## 5.2. Repeating Widely Separated Events

A unique characteristic of some PPISNe is their ability to produce violent explosions separated by decades, or even millennia of quiescent, star-like behavior (Woosley 2017). Much has been made of the possibility that the same star that produced SN 1961V might still be “alive” decades later or even now. Occasionally, that possibility has been used to argue against a SN origin for the main event (Van Dyk & Matheson 2012). Conversely, the presence of a strong radio or x-ray source has been taken as evidence that a real SN happened (Chu et al. 2004), and that the star must therefore be gone. Both arguments are potentially specious if a star can explode violently as a SN more than once.



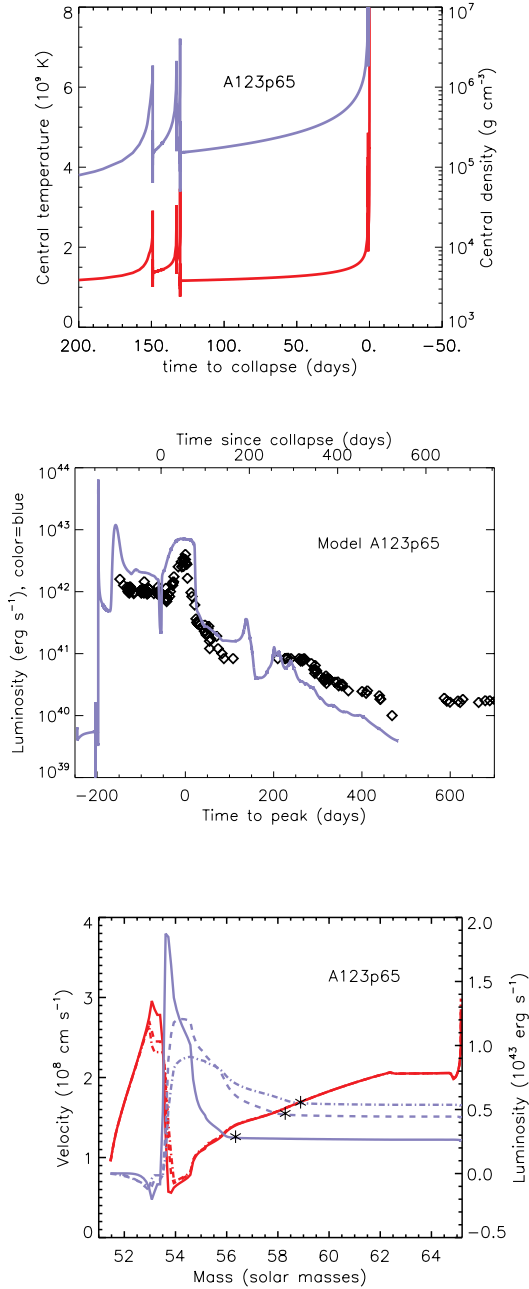


FIG. 6.— (top:) Pulsing history of Model A123p65. The central temperature and density are shown as a function of time to core collapse. A weak pulse ( $T_p = 2.91$  GK) at 149.1 days before collapse launches a shock that unbinds most of the envelope. Two stronger closely separated pulses at 132.8 days ( $T_p = 3.05$  GK) and 130.3 days ( $T_p = 3.46$  GK) illuminate the previously ejected material. Finally a series of three rapid pulses 0.977, 0.958 and 0.925 days ( $T_p = 4.04, 4.25$  and  $4.86$  GK) leads to a terminal brightening just as the core collapses to a black hole (the brightening is delayed from the time of pulses because of diffusion time). (middle:) Comparison of the bolometric light curve of Model A123p65 with that estimated for SN 1961V. Time is plotted relative to the observed peak for SN 1961V on the bottom axis and to core collapse on the top axis. The single observed point at -366 days is omitted in this plot as are observations beyond 700 days postpeak. (bottom:) Radiation transport in Model A123p65. The velocity (red) and luminosity (blue) are shown as a function of mass for three different times, 10 d (solid), 20d (dashed), and 25 d (dash-dotted) after core collapse (see the time scale on the top of the middle panel). Note the diffusion of light ahead of the shock. Asterisks indicate location of the electron scattering photosphere.

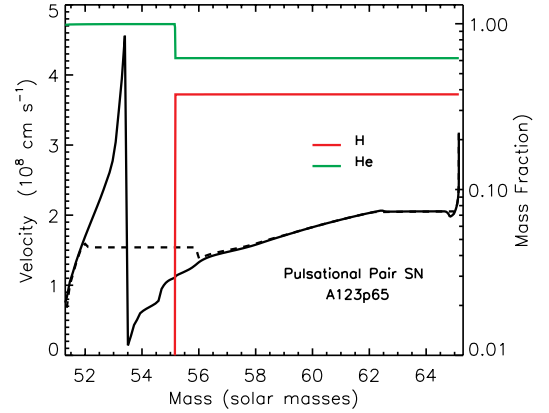


FIG. 7.— Velocity (black line) and ejected H/He composition for Model A123p65 as a function of mass. The velocity at the time of iron-core collapse (solid line) and at 700 days (dashed line) are shown. The photosphere is just outside of the high velocity material in the pre-SN star. Velocities in the hydrogen-rich material range from 1500 to 2100  $\text{km s}^{-1}$ , except for a small amount of high velocity material ( $\sim 3,000$   $\text{km s}^{-1}$ ) at the outer edge. The plot for Model A123p7 would be similar, but the final velocities are about 15% greater.

Fig. 8 shows two examples. Both are of the low carbon variety, TH114p25 and TH115p25. It is possible to find examples among the high-carbon models, e.g. A140p6, that have a similar history and initial light curves comparable in luminosity and duration to SN 1961V, but, in this limited survey, none was found with more than one pulse in the initial outburst. Single-pulse events end up looking like ordinary PISNe (Fig. 2) and were excluded.

The light curves for TH114p25 and TH115p25 in Fig. 8 are really just the first outbursts of these models. Model TH114p25 was a SN again and finally collapsed to a black hole 40 years later (i.e., in 2001). Model TH115p25 did the same thing 106 years later (i.e., in 2067). No great weight should be given to these specific dates, but the implication is that the progenitor of SN 1961V might or might not still be there and that it could still die at anytime. The second events are probably not very bright optically. They eject no hydrogen or radioactivity, and the hydrogen shells from 1961V itself are now out at  $4 \times 10^{17}$  cm, so any interaction is likely to be long, faint, and not optically efficient.

The speeds of the hydrogen-rich ejecta in these models are again close to  $2000$   $\text{km s}^{-1}$  after 1961 (Fig. 9), and each eventually makes a black hole of  $46 M_{\odot}$ . These models have the additional merit over those of § 5.1 or § 5.3 of explaining the years of post-1961 emission of SN 1961V. The remaining star was greatly inflated by the initial explosion. The central density and temperature of the  $49.9 M_{\odot}$  remnant of Model TH115p25 after its first couple of pulses are  $2.6 \times 10^4$   $\text{g cm}^{-3}$  and  $0.697$  GK. The long lifetime of the stellar remnant is because this is near the temperature where neutrino losses become less efficient than radiative losses. The photosphere of the remaining star is almost entirely helium. Indeed the hydrogen-poor photosphere of the remaining star is a characteristic of any SN origin for the main event. Van Dyk & Matheson

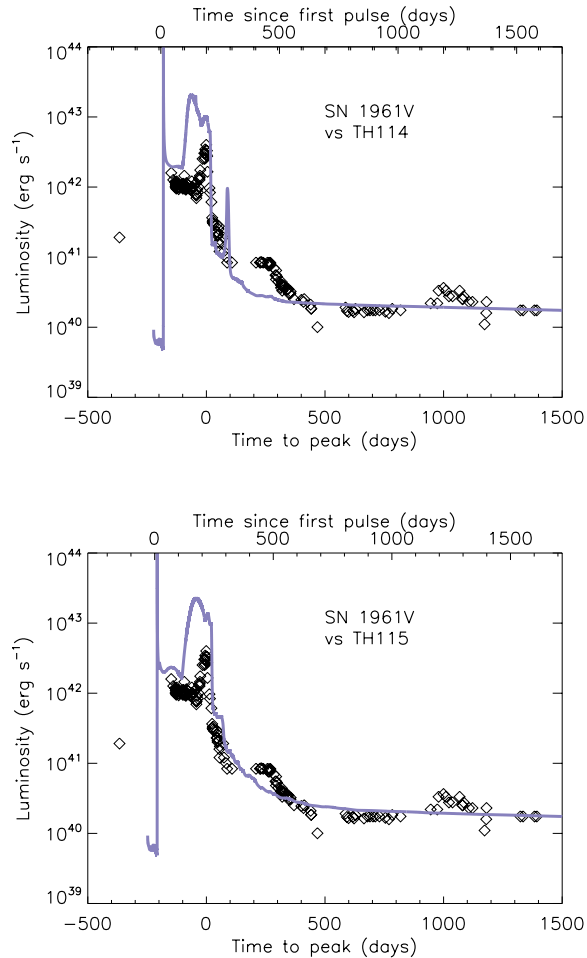


FIG. 8.— (top:) The early bolometric light curves of Models TH114p25 and TH115p25 compared with SN 1961V for the 4.5 years when the SN was well observed. Time for the model is measured since the first pulse (top axis) and for the SN relative to the time of its observed peak luminosity (bottom axis). The model luminosity prior to  $t = 0$  is the pre-SN star. Emission after about 500 days is from the residual stars, both of which retain a mass at this point of  $50 M_{\odot}$ . The overall light curve of SN 1961V is in good agreement with this model, though not the initial observed point at  $-366$  days, which must have other causes. In Model TH115p25, a stellar remnant would still be shining at approximately the Eddington luminosity ( $\sim 10^{40} \text{ erg s}^{-1}$ ) today, but for Model TH114p25 the star died around 2001.

(2012) claimed that 61V was “alive” based on a lingering source (Object 7) that had  $H\alpha$  emission like an LBV wind, but any survivor of the 1961 explosion would not have a hydrogen envelope anymore.

During the long wait before its final collapse, the star contracts, with no nuclear burning, and radiates near the Eddington luminosity,  $\approx 1 \times 10^{40} \text{ erg s}^{-1}$ . There may be small additional contributions from (Eddington-limited) accretion from fallback and circumstellar interaction with a wind, but a persistent luminosity near  $10^{40} \text{ erg s}^{-1}$  seems guaranteed for many decades. The emission properties of the central star are difficult to predict due to fallback, the contraction of the still hot outer layers of the protostar-like object, and the possible interaction of any radiation with the SN ejecta, but it would

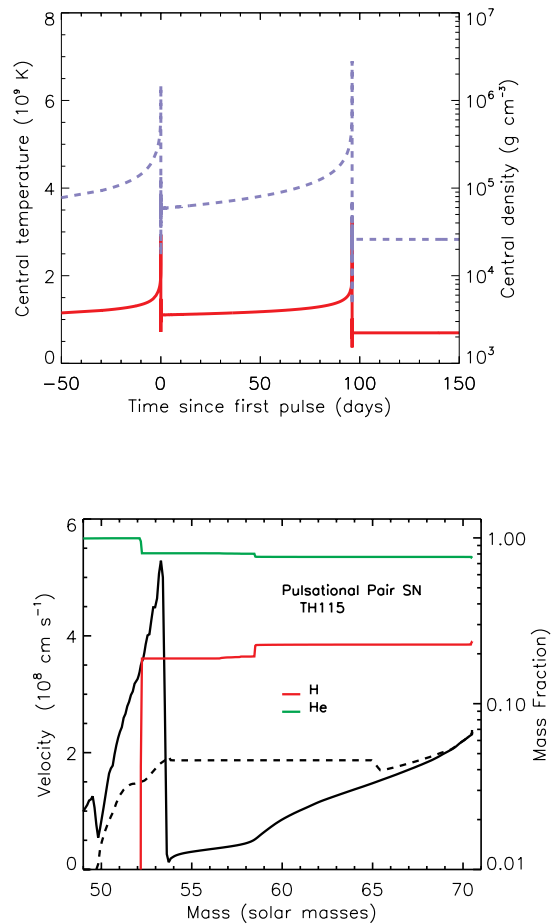


FIG. 9.— (top:) Pulsing history of Model TH115p25 during the first series of pulses. Additional events occurred 106 years later, culminating in the collapse of the core to a black hole. Central temperature and density are plotted vs time since the first pulse. The first pulse ejected the hydrogen envelope, producing a low-energy SN II-P. The second pulse ejected matter that interacted with the prior ejecta to produce the late peak in the light curve. (bottom:) The velocity and composition profile for Model TH115p25 at a time just before peak (solid line) and much later when the luminosity has declined to  $10^{41} \text{ erg s}^{-1}$ . The high velocities at the earlier time are well beneath the photosphere.

be very hot with a radius of order  $10^{12} \text{ cm}$  and effective temperature  $\sim 50,000 \text{ K}$ . Without a hydrogen envelope, this luminous contracting He star would resemble a very luminous Wolf-Rayet star, and may be faint in optical images despite its high bolometric luminosity. Recent limits on bolometric luminosity, including any non-optical mission (especially deep UV observations), substantially less than  $10^{40} \text{ erg}$  would rule out models like TH115p25 that still survive as a star today, but would not constrain models that already died like TH114C.

### 5.3. Enduring Explosions

There is a third class of models in which violent pulsations persist for several years, but not decades, and SN 1961V happened to be caught in the later stages of the star’s death. These models have very irregular light curves, resulting from multiple colliding shells with var-

ious speeds and masses, and obtaining a good match to SN 1961V is difficult. In all these cases, there would need to have been an earlier bright transient, comparable to the brightness of the main peak in late 1961, that occurred before the plateau phase of SN 1961V, but was not observed. Examples of this class are Models TH109p25 and A126p65 (Table 3; Fig. 10 and Fig. 11). The core in these models explodes several times. For TH109p25 there were three pulses that happened 594 d, 358 d, and 250 d prior to core collapse. The central temperature, after oscillations following the first pulse damped, was 1.03 GK and after the second pulse, 1.15 GK. These temperatures set the waiting time for the next pulse to be 236 and 108 days, which is about the time for matter moving at  $2000 \text{ km s}^{-1}$  to coast to a few times  $10^{15}$  cm and become optically thin. This gives rise to pronounced, multi-peak light curves that are not as smooth as other models. Much greater time or speed, and the collisions would happen outside  $10^{16}$  cm where the optical efficiency might be less and the collision times longer. Much less and there would just be one continuous event like in § 5.1. Similarly, in Model A126p65 there were also three major pulses (Fig. 11) prior to core collapse: a single weak pulse 381 days before collapse (subsequent central temperature 1.04 GK); a double pulse at 33.2 d and 30.1 d (subsequent central temperature 1.42 GK) and a final pulse 0.85 days before core collapse.

The broad peaks in both Models TH109p25 and A122p65 before core collapse are, as usual, due to individual pulses charging overlying optically thick matter with radiation that then diffuses out, but the narrow peaks after -150 days (relative to peak) result from colliding shells at lower optical depth. The narrow 30 day peak of SN 1961V in both models, results from “circumstellar interaction”, not diffusion and recombination or radioactivity. Its spectrum might thus be novel. As remarked previously (§ 5.1), these narrow spikes in emission should actually be fainter and broader because of multidimensional instabilities not followed in KEPLER.

Still, the timing and qualitative agreement, especially of Model A126p65, with SN 1961V for over 500 days of emission is impressive. The late time emission comes from continuing shock interaction, and could, of course, be enhanced further if there was large mass loss due to precursor LBV-like variability, as noted earlier. In Model TH109p25, there is an additional collision of shells about 1000 d after peak. Once again this peak should be broader and fainter because of multi-dimensional effects. Crudely, one might expect the thin shell to have been spread over a region with thickness  $\Delta r/r \sim 10 - 20\%$  (Chen et al. 2016) and the peak in the light curve broadened by a comparable amount,  $\Delta t/t \sim 10 - 20\% \sim 150$  d. Repeated outbursts on the tail of up to 1 mag were reported by (Bertola & Arp 1970).

Both these models also offer the possibility of explaining the brightening one year before peak. Model TH109p25 accidentally passes right through that point. In Model A126p65, an explosion had already occurred, but the bolometric light curve had already fallen to an order of magnitude fainter than the pre-SN limit. CSM interaction of the leading shock with the pre-SN wind might explain the discrepancy.

In any case, CSM interaction would need to be invoked in both these models to explain the very late-time emis-

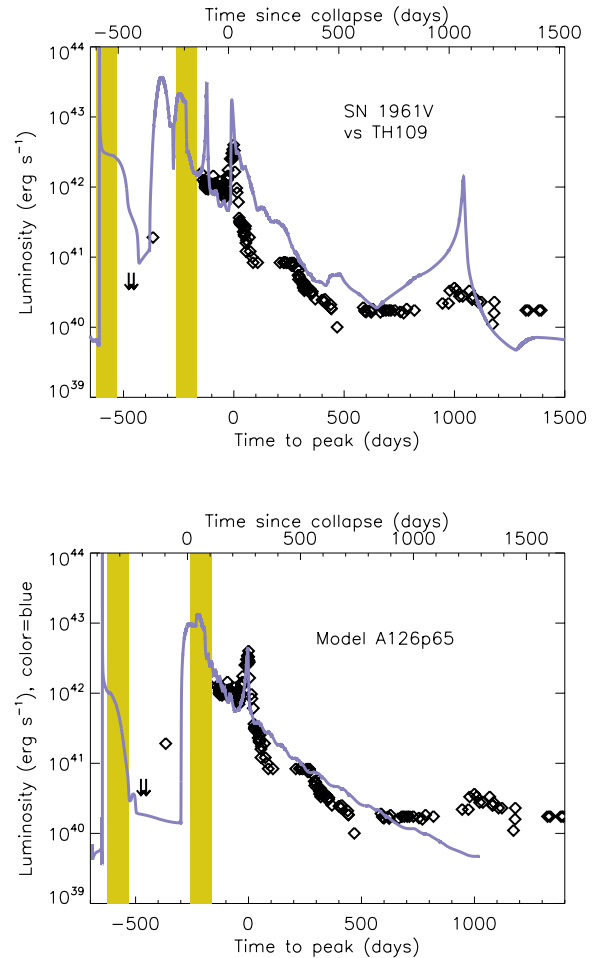


FIG. 10.— Comparison of the bolometric light curves of Models TH109p25 and A126p65 with observations of SN 1961V. The model luminosities have a complex structure resulting from both repeated explosions and shell collisions. The models predict bright prior events that might have escaped detection. Note that days  $-260$  to  $-165$  and  $-625$  to  $-530$  relative to peak (vertical gold bands) are when SN 1961V is not observable due to R.A. constraints (§ 5.4). Upper bounds on the luminosity at  $-453$  and  $-476$  days before peak can be problematic depending on the spectrum and exact timing of pulses. At time zero on the top axis the core collapses to a black hole and is removed from the calculation. Very late time emission might be augmented by interaction with a pre-SN stellar wind.

sion after 1000 days. An increasingly uncertain bolometric correction must also be applied at these late times, so the actual luminosity may need to be larger to explain what was seen in optical wavelengths.

#### 5.4. Absence of Evidence for Pre-supernova Supernovae

Some of the model light curves that most closely resembled SN 1961V also had “pre-SN” emission as bright as the main event in SN 1961V that were, unfortunately, not observed. In some cases these bright peaks came shortly before discovery of SN 1961V at a time when data was missing or sparse. Remarkable examples are the bright initial peaks seen in the “single-event” model A123p65 discussed in § 5.1 (Fig. 6), as well as the “enduring explosion” models TH109 and A126p65 discussed in § 5.3 (Fig. 10).



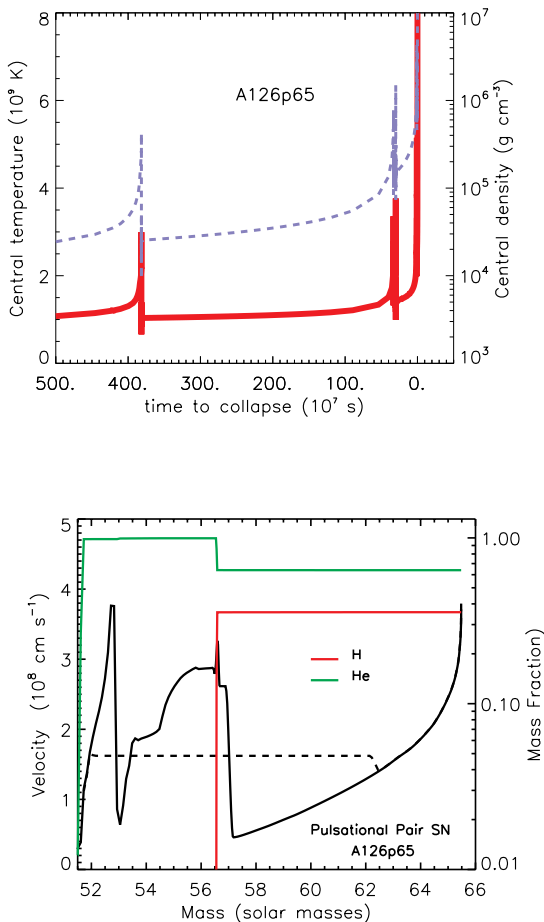


FIG. 11.— (top:) The pulse history for A123p65 shows three pulses plus a final collapse to a black hole. (bottom:) ejected composition and velocity for the same model. The solid line shows the velocity at the time of core collapse with high values due to the terminal pulses shown in the top plot. The dashed line shows the velocity years later at the last point plotted in Fig. 10.

Without a more detailed examination of archival plates or observing logs, and without entering the minds of observers at the time, it is difficult to ascertain the implications of the lack of data. At the present time, with multiple ongoing professional and amateur SN searches scouring the sky, it would be difficult to believe that such a bright event would be missed. For a bright event in 1960, however, things could have been different.

In this regard, it is worthwhile to examine the observability of SN 1961V. For its location at R.A.  $\approx 2.4h$  and DEC  $\approx +37^\circ$ , SN 1961V was close to the Sun and at high airmass ( $>2$ ) for northern hemisphere observatories from late March until early July. These dates translate roughly to a time period from day  $-260$  until day  $-165$  relative to the main peak in November 1961. Indeed, SN 1961V was discovered on July 11, 1961 (Wild 1961), just after it had emerged from behind the Sun, and the last pre-SN observation was long before day  $-260$  at day  $-366$  relative to the peak. Therefore, if a very bright early peak occurred shortly before discovery (as in models TH109 and A126p65 in Fig. 10), it would have been

very difficult or impossible to observe. For this reason, we conclude that the PPISN model light curves shown in Figures 6 and 10, which are predicted to have bright but unobserved early peaks during this time period, provide viable explanations for SN 1961V.

Model A126p65 also shows another previous bright peak almost 2 years before the November 1961 peak. During that time frame, the previous period when SN1961V was unobservable was at day  $-625$  to day  $-530$  relative to peak; it is perhaps bad luck that this almost exactly coincides with the first luminosity peak of Model A126p65 in Figure 10, prohibiting it from being observed.

We also note two reported observations of the source at SN 1961V’s position on 1960.641 and 1960.704 (see Table 1), which we choose to plot as upper limits in Figure 10 at days  $-476.3$  and  $-453.3$ . These points would seem to disfavor model TH109, as they are somewhat below the predicted luminosity at that time. We caution the reader, however, not to interpret these upper limits too rigorously. These points come from a private communication from P. Wild, as recounted by Bertola (1963), stating only that the source was “about 17 mag to 18 mag” on those dates. However, no information about the weather or seeing is available, nor the wavelength response of the emulsion used, and this may have been near the limiting magnitude of the 16-inch Bern Observatory Schmidt telescope used by Wild. As such, SN 1961V’s progenitor may have been very difficult to distinguish from its surrounding association. We prefer to interpret these reports as loosely indicating that SN 1961V was not extremely bright at that time.

## 6. CONCLUSIONS

If SN 1961V was a star over  $100 M_\odot$  that exploded as a SN, the most likely explosion mechanism was thermonuclear, brought on by pair instability. The large iron core masses and shallow density gradients at their edges are unfavorable for neutron star production in such massive stars (e.g., Rahman et al. 2021). A collapsar-powered explosion or a millisecond magnetar would require an unusually large amount of rotation for a star that retained its hydrogen envelope, but had also suffered extensive mass loss. While some combination of pair instability and black hole accretion at a low level after the main event is not ruled out, and might even be necessary to explain the sustained emission, we have focused here on “pure” pair-instability models.

An ordinary PISN, one where the entire star explodes in a single pulse, could explain the approximate luminosity, duration, and velocities observed in SN 1961V (§ 4 and Fig. 2), and at least the star would reliably blow up. But PISN are too bright if they last long enough, and too brief if they are faint enough (Fig. 2). With total kinetic energies approaching  $10^{52}$  erg (Table 2), these models also struggle to keep most of hydrogen moving slower than  $2100 \text{ km s}^{-1}$ . PISN models place an interesting limit on the progenitor of SN 1961V though. Even for nuclear reaction rates optimized to require large masses, the progenitor was not more than  $160 M_\odot$  on the main sequence; and had a helium core mass, when it died, of less than  $77 M_\odot$ . The bolometric pre-SN luminosity was therefore less than  $1.4 \times 10^{40} \text{ erg s}^{-1}$ . No model in this paper that looked at all similar to SN 1961V had a greater main sequence mass or pre-SN luminosity. When

examined closely though, a PISN origin for SN 1961V seems unlikely. Better agreement can be achieved using pulsating models.

Three classes of PPISN models were explored. In the simplest case, SN 1961V was a single event that happened in 1961 (§ 5.1). Its light curve was powered by repeated flashes in quick succession, but the iron core collapsed before the brightest emission (i.e., before the observed flare that peaked on day 1961.943 in Table 1) began. This kind of model resembles those for ordinary SNe II where the energy from neutron star formation is all deposited centrally within a few seconds, but it differs in that the central energy source repeats discontinuously throughout the light curve. That energy can also be significantly augmented, at late times, by colliding shells (Fig. 4 and Fig. 6). These variations imprint themselves on the light curve.

Reasonably good fits to the bolometric light curve and velocity were obtained for a variety of single-event models (Fig. 4 and Fig. 5), but the best fits were for models with one-third solar metallicity, high carbon abundance, relatively small radii, a helium core mass of about  $55 M_{\odot}$ , and a hydrogen envelope of about  $10 M_{\odot}$  - Model A123p65 (Fig. 6, Fig. 7, and Table 3). Six hundred days of bolometric emission are replicated to about a factor of two. Excess emission at late times (around 300 days post-peak) could naturally be attributed to interaction of a few hundredths of a solar mass of ejecta with a speed of  $2500 \text{ km s}^{-1}$  crashing into a pre-SN wind of only  $0.001 M_{\odot} \text{ y}^{-1}$ , or perhaps alternatively to black hole accretion. Emission one year prior to peak must find another explanation, but the star was rapidly adjusting its central structure then and may have been an LBV (§ 3.1).

Other variations on the PPISN theme also give impressive matches to observational data. In the second class of models, SN 1961V was one of two widely separated SNe (Fig. 8 and Fig. 9), although the second might not have been a bright optical event. More work on the emission properties of shocks in dense media with a radius of  $\sim 10^{17}$  is needed. Here the low-carbon models seem to have an advantage in that explosive oxygen burning commences promptly and can, with some searching in model space, set up conditions for a more powerful second pulse  $\sim 100$  days later. After this, there ensues a long wait while the star recovers in a protostar-like contraction phase, experiencing Kelvin-Helmholtz evolution as it emits at about the Eddington luminosity. This hot “protostar” may have disappeared into a black hole after a few decades or could still be there. Its luminosity, integrated across all wavelengths, would remain close to  $10^{40} \text{ erg s}^{-1}$ . Two deficiencies of the model are that it does not explain the emission one year before peak, and that the maximum is too broad and bright (Fig. 8).

In the third class of models (§ 5.3), SN 1961V was only a piece of a longer and probably much brighter SN that went largely unobserved (Fig. 10 and Fig. 7) before July 1961. The narrow width of the peak here is attributed to the collision of geometrically thin shells. Continuing interaction between shells can keep the SN bright for years, although ultimately some sort of interaction with a pre-SN wind would also contribute. This model, uniquely, allows for the existence of bright emission related to pulsational activity a year before the main event.

None of these models is perfect. Most of the single-

event models are too bright (e.g., Fig. 6 and Fig. 8). They emit too much light both at peak and integrated over time. A possible exception might be Model A123p65 (Fig. 6). That model works if about 40 days of bright emission was missed prior to the SN’s discovery, but SN 1961V was actually unobservable during that time period, making this a very plausible model (§ 5.4). A still weaker explosion than  $4 \times 10^{50} \text{ erg}$  might also help. Compare the integrated light output in the observed  $\sim 1000$  day event (Table 1), which is about  $2.4 \times 10^{49} \text{ erg}$ , with the higher 1000 day bolometric light output of the models (Table 3). Part of the discrepancy is that the observations may have missed some early bright phases of the model’s light curve. Again, though, SN 1961V was unobservable or difficult to observe before its discovery in July 1961, making this also a plausible model. Another is that observers at the time generally reported photographic (blue sensitive) magnitudes, not bolometric magnitudes, and so there still might be a problem at the factor-of-two level. Finally, the models are 1D and nature is not, and so very sharp luminosity spikes or dips in the models are likely to be somewhat smoother in reality.

The brightest peak in the single event models is also broader than in the observations. This could reflect too large an envelope mass. A mass less than the  $10 M_{\odot}$  ejected by Model A123p65 would have a shorter diffusion time and could still satisfy velocity constraints, but Model A123p7 (not illustrated) had difficulty sustaining steady emission for 150 days. A perfect single-event fit, or even one better than the two shown in Fig. 6, has been elusive. Perhaps this speaks in favor of long complex events like Fig. 10, but implies a very bright SN prior to July, 1961.

What can be done to clarify this situation and discriminate among the three sets of models? Most straightforward, though not easy, nuclear cross section measurements could refine the carbon abundance expected for such massive stars after helium burning. Here it is a parameter. In nature, it is not. Better treatments of radiation transport can clarify the spectrum and bolometric correction for each successful model. This might not be as easy as it seems, since one cannot assume a coasting configuration when shock waves are being repeatedly launched and shells are colliding. Most advanced radiation transport codes, so far, assume a coasting configuration. Observational studies of the remnant might discover, or rule out the tens of solar masses of slow moving oxygen expected in the PISN models or even in ordinary SNe. The debate about whether there is still a star-like object in the site of SN 1961V can continue, but perhaps with a different interpretation, since a surviving star and a SN are not incompatible. Searches for high-energy emission from a newly formed  $50 M_{\odot}$  black hole with luminosity near the Eddington limit might also be carried out. A better understanding of the physics involved in LBVs is needed in order to address the precursor variability and mass loss. Rotating PPISN models might be considered as a way of potentially further weakening the pair instability (Marchant & Moriya 2020; Woosley & Heger 2021).

If SN 1961V was indeed a pulsational SN, there are many interesting implications for stellar evolution. First, it would confirm that PPISN do actually happen in na-

ture, and that uncertain mass loss and reaction rates do not conspire to rule out their existence. Events like SN 1961V are rare, but they also sample a narrow range of masses, with helium cores near  $50 M_{\odot}$ . Other varieties of PPISN (and PISN) should also exist and be sought (Woosley 2017). The inferred low metallicity for the SN 1961V site (one-third solar?) suggests a metallicity dependence in mass-loss rate that may favor the preservation of very high mass at death, which is consistent with modern reductions in mass-loss rate prescriptions. For a roughly  $110 M_{\odot}$  star with  $1/3 Z_{\odot}$  to die with a mass of  $\sim 60 M_{\odot}$  is informative. Finally, this would indicate that a likely route exists for producing black holes around  $40\text{-}50 M_{\odot}$ , many of which have been found by LIGO.

While the emphasis here is on SN 1961V, we are aware

that other similar events, e.g., SN 2009ip (Mauerhan et al. 2013; Pastorello et al. 2013), have been observed and even attributed to PPISN. We save the modeling of these events for another day, but note in passing that the high velocities observed in SN 2009ip, both before and during the 2012 outbursts, may be difficult to accommodate in a PPISN framework without additional embellishments. We doubt that all “supernova impostors” are PPISNe, because pair instability supernovae are too infrequent and SN 1961V was unusually luminous and energetic, but we hope to have made a compelling case at least one was.

#### REFERENCES

- Abbott, B. P., Abbott, R., Abbott, T. D., et al. 2019, *Physical Review X*, 9, 031040.
- Barkat, Z., Rakavy, G., & Sack, N. 1967, *Physical Review Letters*, 18, 379
- Bertola, F. 1964, *Annales d’Astrophysique*, 27, 319
- Bertola, F. 1963, *Contrib. Asiago*, 142, 13
- Bertola, F. & Arp, H. 1970, *PASP*, 82, 894.
- Branch, D., & Greenstein, J. 1971, *ApJ*, 67, 89
- Branch, D. & Cowan, J. J. 1985, *ApJ*, 297, L33.
- Chen, K.-J., Woosley, S. E., & Sukhbold, T. 2016, *ApJ*, 832, 73.
- Chevalier, R. A. 1982, *ApJ*, 259, L85
- Chu, Y.-H., Gruendl, R. A., Stockdale, C. J., et al. 2004, *AJ*, 127, 2850.
- Ensmann, L. 1989, *BAAS*
- Dessart, L. & Hillier, D. J. 2011, *MNRAS*, 410, 1739.
- Dessart, L., Hillier, D. J., Waldman, R., et al. 2013, *MNRAS*, 433, 1745.
- Farmer, R., Renzo, M., de Mink, S. E., et al. 2019, *ApJ*, 887, 53
- Farmer, R., Renzo, M., de Mink, S., et al. 2020, *ApJ*, 902, L36.
- Filippenko, A. V., Barth, A. J., Bower, G. C., et al. 1995, *AJ*, 110, 2261.
- Gilmer, M. S., Kozyreva, A., Hirschi, R., et al. 2017, *ApJ*, 846, 100
- Goldberg, J. A., Jiang, Y.-F., & Bildsten, L. 2021, *arXiv:2110.03261*
- Goodrich, R. W., Stringfellow, G. S., Penrod, G. D., & Filippenko, A. V. 1989, *ApJ*, 342, 908
- Heger, A. & Woosley, S. E. 2002, *ApJ*, 567, 532
- Heger, A., Fryer, C. L., Woosley, S. E., et al. 2003, *ApJ*, 591, 288
- Humphreys, R. M., Davidson, K., & Smith, N. 1999, *PASP*, 111, 1124.
- Jiang, Y.-F., Cantiello, M., Bildsten, L., et al. 2018, *Nature*, 561, 498
- Kasen, D., Woosley, S. E., & Heger, A. 2011, *ApJ*, 734, 102
- Kochanek C. S., Szczygiel D. M., Stanek K. Z., 2011, *ApJ*, 737, 76
- Kochanek C. S., Szczygiel D. M., Stanek K. Z., 2012, *ApJ*, 758, 131
- Lodders, K. 2003, *ApJ*, 591, 1220
- Marchant, P. & Moriya, T. J. 2020, *A&A*, 640, L18
- Mauerhan J.C., et al. 2013, *vMNRAS*, 430, 1801
- Nieuwenhuijzen, H., & de Jager, C. 1990, *A&A*, 231, 134
- Pastorello, A., Cappellaro, E., Inzerra, C., et al. 2013, *ApJ*, 767, 1
- Patton, R. A., Kochanek, C. S., & Adams, S. M. 2019, *MNRAS*, 489, 1986.
- Paxton, B., Schwab, J., Bauer, E. B., et al. 2018, *ApJS*, 234, 34
- Rahman, N., Janka, H.-T., Stockinger, G., et al. 2022, *MNRAS*, in press, *arXiv:2112.09707*
- Sanyal, D., Grassitelli, L., Langer, N., and Bestenlehner, J. M., 2015, *A&A*, 580, A20
- Schaerer, D., Meynet, G., Maeder, A., et al. 1993, *A&AS*, 98, 523
- Shiode, J. H. & Quataert, E. 2014, *ApJ*, 780, 96.
- Smith, N., Gehrz, R. D., Hinz, P. M., et al. 2003, *AJ*, 125, 1458
- Smith, N., Vink, J.S., & de Koter, A. 2004, *ApJ*, 615, 475
- Smith, N., & Owocki, S. 2006, *ApJ*, 645, L45
- Smith, N., Chornock, R., Silverman, J. M., Filippenko, A. V., & Foley, R. J. 2010a, *ApJ*, 709, 856
- Smith, N., Miller, A., Li, W., et al. 2010b, *AJ*, 139, 1451
- Smith, N. 2011, *MNRAS*, 415, 2020
- Smith, N., Li, W., Silverman, J. M., Ganeshalingam, M., & Filippenko, A. V. 2011, *MNRAS*, 415, 773
- Smith, N. 2014, *ARA&A*, 52, 487
- Smith, N., Andrews, J. E., Rest, A., et al. 2018, *MNRAS*, 480, 1466
- Sukhbold, T., Ertl, T., Woosley, S. E., et al. 2016, *ApJ*, 821, 38
- Utrobin, V. P. 1984, *Ap&SS*, 98, 115
- Van Dyk, S. D., Filippenko, A. V., & Li, W. 2002, *PASP*, 114, 700.
- Van Dyk, S. D. & Matheson, T. 2012, *ApJ*, 746, 179.
- Weaver, T. A., Zimmerman, G. B., & Woosley 1978, *ApJ*, 225, 1021
- Wellstein, S., & Langer, N. 1999, *A&A*, 350, 148
- Wild, P. 1961, *I.A.U. Circ. No. 1764*.
- Woosley, S. E., Heger, A., & Weaver, T. A. 2002, *Reviews of Modern Physics*, 74, 1015
- Woosley, S. E., Blinnikov, S., & Heger, A. 2007, *Nature*, 450, 390
- Woosley, S. E. 2017, *ApJ*, 836, 244.
- Woosley, S. E. & Heger, A. 2021, *ApJ*, 912, L31.
- Zwicky, F. 1964, *ApJ*, 139, 514